Neurochemical Research (2019) 44:2239–2260
https://doi.org/10.1007/s11064-018-2611-y

ORIGINAL PAPER

Metabolomic Assays of Postmortem Brain Extracts: Pitfalls in Extrapolation of Concentrations of Glucose and Amino Acids to Metabolic Dysregulation In Vivo in Neurological Diseases

Gerald A. Dienel[1,2]

Received: 1 May 2018 / Revised: 5 August 2018 / Accepted: 6 August 2018 / Published online: 16 August 2018

Abstract

Glucose utilization is reduced in vulnerable brain regions affected by neurological disorders, especially Alzheimer's disease (AD), but the basis for abnormal glucose homeostasis is unknown. Studies of brain-bank human tissue have made major contributions to understanding complex aspects of neurological, psychiatric, and neurodegenerative diseases, but they are not appropriate for metabolomic analysis of labile metabolites because postmortem intervals between death and tissue freezing are much too long. Recent reports of postmortem brain glucose levels led to suggestions that AD patients may be hyperglycemic and that elevated brain glucose levels along with reduced glycolytic activity reveal abnormal glucose homeostasis before clinical symptoms become manifest. These conclusions are, however, questioned because virtually all brain glucose is consumed within minutes after death, followed by progressive increases in glucose and amino acid levels, presumably due to autolytic changes. To illustrate pitfalls in use of autopsy material for metabolomic assays of labile metabolites, data from living human brain are compared with those from autopsy samples, and metabolism at the onset of postmortem ischemia is compared with calculated glycolytic enzyme activities. Postmortem glucose levels range from extremely low to unrealistically high, precluding their extrapolation to living brain. Indirect evaluation of glycolytic enzyme activities in postmortem AD brain is not valid because the glucose and amino acid concentrations used in the calculations are not stable after death, and reported values are unrealistically high. Specific recommendations are provided for non-invasive longitudinal monitoring of brain metabolism and metabolite levels in patients with neurological diseases.

Keywords Alzheimer's disease · Autolysis · Glucose · Amino acids · Glycolysis · Postmortem ischemia

Abbreviations

AD	Alzheimer's disease
Ala	Alanine
CMR_{glc}	Rate of glucose utilization
fMRI	Functional magnetic resonance imaging
Glc	Glucose
Glc-6-P	Glucose-6-phosphate
GLUT	Glucose transporter
Gly	Glycine
HK	Hexokinase
MRS	Magnetic resonance spectroscopy
PCr	Phosphocreatine
PFK	Phosphofructokinase
PK	Pyruvate kinase
Ser	Serine
TCA	Tricarboxylic acid

✉ Gerald A. Dienel
gadienel@uams.edu

[1] Department of Neurology, University of Arkansas for Medical Sciences, 4301 W. Markham St., Slot 500, Little Rock, AR 72205, USA

[2] Department of Cell Biology and Physiology, University of New Mexico, Albuquerque, NM 87131, USA

Introduction

Glucose is the obligatory fuel for brain, and glucose utilization rates (CMR_{glc}) vary regionally in normal resting brain, with local increases during activation and decreases when neural activity is reduced [1]. CMR_{glc} is, therefore, often used as a surrogate to evaluate functional activity and consequences of disease in different brain regions. [^{18}F] Fluorodeoxyglucose positron-emission tomographic (FDG-PET) assays measure total CMR_{glc} in living brain at the hexokinase (HK) step, the first irreversible reaction of the

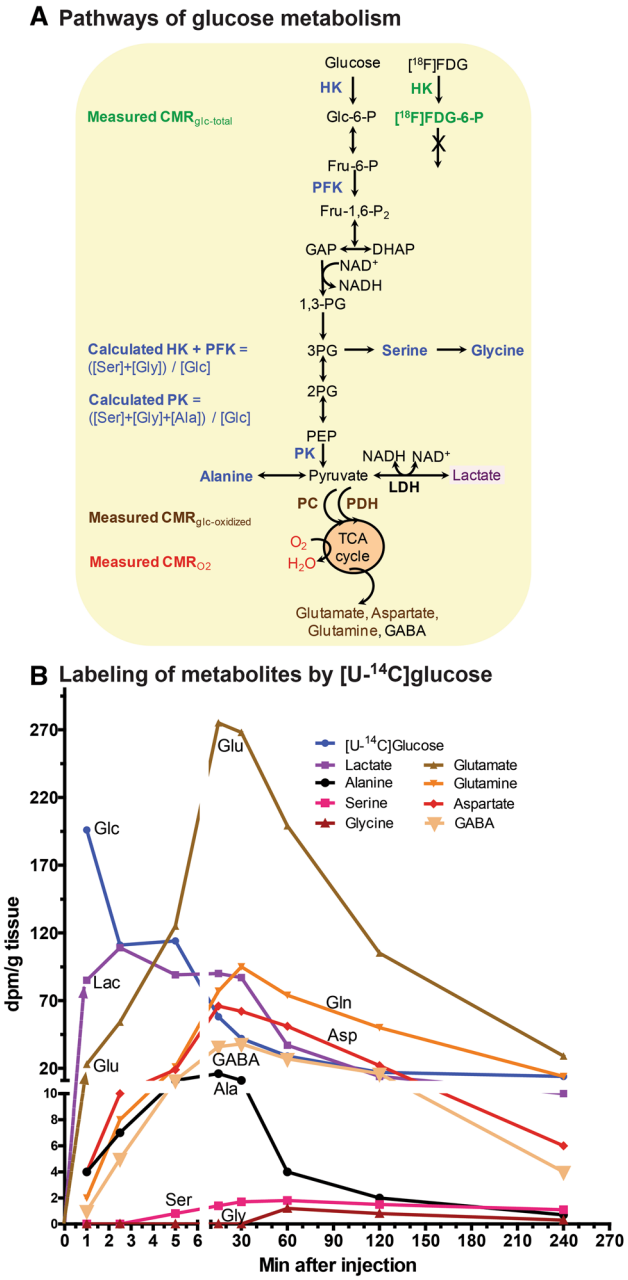

Fig. 1 Pathways and labeling of metabolites by [U-^{14}C]glucose. **a** ▶ Metabolism of labeled glucose (Glc) via the glycolytic and tricarboxylic acid (TCA) cycle pathways results in labeling of pathway intermediates and amino acids at different steps. [^{18}F]Fluorodeoxyglucose (FDG) is used in positron-emission tomographic (PET) studies to measure cerebral metabolic rate (CMR) of total glucose utilization ($CMR_{glc\text{-}total}$) at the hexokinase (HK) step because FDG-6-P is trapped in the cell where it was phosphorylated and not further metabolized via the glycolytic pathway. Phosphofructokinase (PFK) is a key regulatory enzyme of the glycolytic pathway. Pyruvate kinase (PK) converts phosphoenolpyruvate (PEP) to pyruvate that can be converted to lactate, alanine, or oxaloacetate, or be oxidized in the TCA cycle. The rate glucose oxidation ($CMR_{glc\text{-}oxidation}$) after entry of pyruvate into the TCA cycle via the pyruvate carboxylase (PC) and/or pyruvate dehydrogenase (PDH) reactions is commonly measured by magnetic resonance spectroscopy (MRS) in conjunction with metabolic modeling by determination of rates of incorporation of [^{13}C]glucose into TCA cycle-derived amino acids during programmed infusions of [^{13}C]glucose to achieve steady state, i.e., constant fractional enrichment of glucose in arterial plasma and brain (reviewed in [4]). Rates of oxygen consumption (CMR_{O2}) can be determined by incorporation of $^{15}O_2$ or $^{17}O_2$ into H_2O with PET or MRS assays, respectively [4]. An et al. [5] proposed a novel approach to indirectly estimate the rates of the HK + PFK and PK reactions, both calculated from ratios of the sum of amino acid concentrations to glucose concentration (see text). **b**. Time courses of labeling of glucose (Glc)-derived amino acids and lactate (Lac) in brain after a pulse intravenous injection of tracer amounts of [U-^{14}C]glucose into awake rats. Pulse labeling causes the concentration of [^{14}C]glucose in brain to quickly reach a peak, then progressively fall as it is cleared from plasma (due to uptake and metabolism by body tissues and metabolism in brain). Concentrations of ^{14}C-labeled metabolites reach peak levels at varying times due to differences in pathway fluxes, then fall as label is cleared from the metabolic pools. In contrast, programmed infusions used in MRS studies keep the concentration of labeled glucose constant, and incorporation of label into glucose-derived metabolites increases progressively until steady state for each isotopomer is attained (not shown: for examples in human and rat brain, see [6, 7]). Dissimilar labeling time courses after pulse and programmed infusions, use of anesthesia in animal subjects, and differences in metabolic rates between rodents and primates may also contribute to variations in the magnitude and time courses of metabolite labeling patterns. Also, [U-^{14}C]glucose labeling reports total ^{14}C in each metabolite, it has high sensitivity, and it can detect rapid labeling of metabolites with low brain concentrations (e.g., *Ser* serine, *Gly* glycine, and *Ala* alanine and Lac). On the other hand, MRS assays are less sensitive and typically focus on the oxidative pathways with measurement of rates of label incorporation into specific carbon atoms (isotopomers) of amino acids derived from the TCA cycle. Note that Ser, Gly, Ala, and Lac are labeled via the glycolytic pathway, and TCA cycle-derived amino acids (*Glu* glutamate, *Asp* aspartate, *Gln* glutamine, and *GABA* γ-aminobutyric acid) are labeled via the oxidative pathways downstream of pyruvate. Plotted from data in Table 1 of Yoshino and Elliott [8]. *Glc-6-P* glucose-6-phosphate, *Fru-6-P* fructose-6-phosphate, *Fru-1,6-P$_2$* fructose-1,6-bisphosphate, *DHAP* dihydroxyacetone phosphate, *GAP* glyceraldehyde-3-phosphate, *1,3-PG* 1,3-diphosphoglycerate, *3PG* 3-phosphoglycerate, *2PG* 2-phosphoglycerate

glycolytic pathway (Fig. 1a). Subnormal CMR_{glc} in vulnerable brain regions of Alzheimer's disease (AD) patients has been firmly established by FDG-PET assays [2], and CMR_{glc} is also reduced, but to a lesser extent, in Huntington's and Parkinson's diseases [3]. However, the FDG method cannot evaluate the downstream metabolic fate of glucose, whereas ^{13}C- and ^{1}H-magnetic resonance spectroscopy (MRS) are used to measure metabolite levels and downstream metabolic pathway fluxes in living brain. MRS approaches have not, however, been used as widely as FDG-PET to study neurological, psychiatric, and neurodegenerative diseases, and substantial knowledge gaps remain. Measurements of metabolite concentrations can help identify pathways affected by diseases, but they do not report fluxes that must be assayed with labeled substrates metabolized by pathways of interest [4] (Fig. 1a).

Postmortem human brain is a valuable resource to evaluate regional anatomical and pathological changes,

and metabolomic, transcriptomic, lipidomic, proteomic, and genomic characteristics of psychiatric and neurodegenerative diseases because animal models do not fully represent all aspects of the diseases (e.g., [37–42]). Postmortem brain does, however, have well-known limitations, including tissue harvest at end-stage of disease, end-of-life agonal states (e.g., cardiovascular or respiratory disorders, fever, low blood flow, hypoxia/ischemia, coma) that can influence tissue integrity and metabolite levels, and autolytic changes during the postmortem interval between death and tissue freezing. Investigators have, therefore, made strong efforts to match age, gender, and postmortem interval for control and disease samples. Relatively short postmortem intervals (median of 3.0 h) are obtained by the Arizona Study of Aging and Neurodegenerative Disorders [43], and characterization of brain RNA integrity and yield from cerebellar cortex revealed negative correlations with postmortem intervals over the range 1.5–45 h, with the best RNA isolates obtained with postmortem intervals < 5 h [44]. Stabilities of proteins are also important and must be established for each protein or enzyme of interest. For example, the in vitro activities of specific glycolytic enzymes are altered in AD [45], and the exact homogenization buffer composition and optimized assay conditions are critical [46]. Fresh surgical brain samples have the highest in vitro activities of phosphofructokinase (PFK), with lower values obtained in frozen-homogenized postmortem tissue, but the specific activity (μmol/min/mg protein) of PFK is stable with respect to postmortem interval prior to freezing, and AD brains have higher PFK activity than matched controls [46]. Determination of postmortem stabilities of compounds of interest in control and diseased tissue is essential to establish the validity of measured values and their interpretation.

In sharp contrast to the relative stability of RNA and protein, energy metabolites (e.g., glucose, glycogen, ATP, phosphocreatine (PCr), and glycolytic and tricarboxylic acid (TCA) cycle intermediates) are extremely labile, being depleted within minutes after death due to ischemia (Box 1). This critically-important issue has been recognized since the 1930s when Kerr et al. carried out a series of pioneering studies establishing that brain glycolytic rate rapidly rises after death, freezing brain in situ with liquid air was required to preserve the actual resting levels of PCr, glucose, glycogen, and lactate, and rapid dissection followed by immediate freezing was inadequate and resulted in substantially lower metabolite levels [33, 47–49]. It is widely recognized in the brain energy metabolism field that special precautions are required to preserve labile metabolites, and rapid freezing or microwave fixation techniques to immediately inactivate brain enzymes, along with rigorous procedures for thawing and extracting the tissue, are routinely used for this purpose [50]. The concentrations of metabolites of interest can then be accurately measured in tissue extracts by various analytical methods.

Box 1. Brain Glucose Concentration and Metabolism in Health and Disease

Living brain glucose transport and metabolism

$$\text{Glucose}_{\text{plasma}} \underset{\textit{transporters}}{\leftrightarrow} \text{Glucose}_{\text{brain interstitial fluid}} \underset{\textit{transporters}}{\leftrightarrow} \text{Glucose}_{\text{brain cells}}$$

$$\rightarrow \text{Glc-6-P} \underset{\textit{glycolysis}}{\rightarrow\rightarrow\rightarrow} \text{Pyruvate} \underset{\textit{oxidation}}{\rightarrow} \text{TCA cycle}$$

$$\text{Pyruvate} \updownarrow \text{Lactate} \leftrightarrow \text{blood}$$

- Glucose transport is equilibrative, driven by concentration gradients
- Normal human brain [glucose] ≈ 1–2 μmol/g, depending on plasma glucose level
- $[\text{Glucose}_{\text{brain}}]/[\text{Glucose}_{\text{plasma}}] \approx 0.2–0.3$
- Brain: plasma glucose equilibration occurs within 1–2 h
- Maximal transport of glucose across the blood–brain barrier ≈ 2CMR_{glc}
- Neurological-neurodegenerative diseases can alter transport and metabolism at many sites

Postmortem brain glucose concentration and metabolism in control and diseased subjects

- Agonal state just prior to death can influence brain metabolite levels
  - Hypoxia, anoxia, hypoglycemia, hypoperfusion
- Blood flow ceases at death
  - Delivery of oxygen and glucose stops
  - Oxidative metabolism halts
  - Ischemia immediately stimulates glycolytic rate many fold
  - Lactate accumulates to about twice [glucose + glycogen]: 2 lactate per glucosyl unit
  - Lactate cannot be washed out of brain
- Rapid depletion of labile energy metabolites: glucose, glycogen, ATP, phosphocreatine
  - Glucose level decreases within seconds, approaches zero within 10–30 min
  - Glycolysis stops when metabolites are depleted

- Key issues
  - Postmortem interval between death and tissue freezing
  - Progressive autolytic changes that alter metabolite concentrations over time
  - Stabilities of different classes of metabolites must be evaluated in control/patient tissue
- Guidelines to avoid pitfalls: quick qualitative checks to detect unreasonable data
  - Absolute metabolite concentrations (not ratios to controls) versus living brain
  - Postmortem brain glucose level versus ante mortem plasma glucose concentration
  - Brain/plasma ratio for glucose versus living brain
  - Calculated metabolic rate or enzyme activities versus living brain

Unfortunately, the rapid postmortem consumption of labile energy metabolites is not appropriately appreciated by scientists and clinicians in other neuroscience disciplines. In fact, altered levels of glucose and other labile compounds determined in cadaver samples with postmortem intervals exceeding 1.5 h have been interpreted in terms of ante mortem hyperglycemia and dysregulation of glucose metabolic pathways prior to death. Studies in postmortem tissue can help guide future research by systems analysis and regional pathophysiology, but longitudinal in vivo brain imaging, MRS, and functional magnetic resonance imaging (fMRI) studies are better suited to quantify metabolite levels, metabolic rates, and metabolic disturbances in neurological disorders.

This article examines the reliability of extrapolation to living brain of energy metabolite concentrations, mainly glucose and lactate, obtained in postmortem human brain samples by reviewing selected studies of neurological diseases. The analysis reveals that published levels of glucose and lactate in postmortem brain determined by capillary electrophoresis-mass spectrometry, gas chromatography–mass spectrometry, or enzymatic assays vary substantially, and most values differ considerably from those in living brain determined by MRS. This discrepancy is not due to methodology per se. Rather, it is due to rapid ischemic changes within seconds due to cessation of blood flow upon death, followed by autolytic processes over longer times prior to tissue freezing and subsequent extraction (Box 1). Calculated enzyme activities based on postmortem levels of glucose and amino acids are proposed to indirectly represent glycolytic enzyme activities, but this approach is also compromised by postmortem changes. Trajectories of plasma glucose levels determined years prior to death were proposed to be predictive of brain glucose level, but correlative forecasts are unlikely to be useful because equilibration of brain and plasma glucose levels can occur within ~ 1 h and postmortem brain levels would be strongly influenced by the agonal state just prior to death.

This review stresses the importance of characterization of energy metabolism in living, not postmortem, brain from three points of view: (i) comparison of in vivo concentrations of labile metabolites in normal subjects and patients with AD to the levels obtained in postmortem brain (Tables 1, 2), (ii) the rapid postmortem decreases in glucose concentration and the slower, progressive increases in levels of glucose and amino acids (Table 3), and (iii) comparison of calculated glycolytic rates with calculated glycolytic enzyme activities (Table 4). Analysis of these data sets reveals avoidable pitfalls in use of brain-bank tissue, and easy ways to evaluate qualitatively the validity of measured brain glucose levels and calculated metabolic rates are provided (Box 1) and discussed. Emphasis is placed on the need for future studies using in vivo studies of brain energetics, pathway fluxes, and labile metabolites.

Concentrations of Glucose and Other Labile Metabolites in Living Human Brain

^{1}H- and ^{13}C-MRS assays and microdialysis techniques enable measurement of selected metabolites in brain tissue and extracellular fluid, respectively, in living brain of normal subjects and in patients with neurological diseases and brain injury.

Take-Home Message

Limited data sets with small AD cohorts suggest that brain glucose levels and brain/plasma ratios for glucose in vivo are elevated above control values, but the increase is modest and not within the hyperglycemic/diabetic range of ~ 4–6 µmol/g.

Ranges of Levels in Normal Brain In Vivo

Extracellular and total glucose concentrations in cerebral cortex of normal awake, non-stimulated, young, middle-aged, and elderly human subjects determined by microdialysis and MRS, respectively, are generally between 1 and 2 µmol/g, with similar levels in cortical gray and white matter and in cerebellum (Table 1). Brain glucose levels vary with arterial plasma glucose concentration due to equilibrative transport, and the brain-to-plasma ratio for glucose is ~ 0.2–0.3 over the range ~ 5–30 mmol/l in plasma when measured by ^{1}H or ^{13}C MRS in living human brain [13, 51, 52]. CMR_{glc} in normal rat brain is about twice that in

Table 1 Concentrations of glucose, lactate, and pyruvate in normal brain of unstimulated, awake human adults in vivo

Mental status	Age (years) mean ± SD or range	Method/brain region	Glucose (μmol/g or ml)	Lactate (μmol/g or ml)	Pyruvate (μmol/ml)	Ratio of [Lactate]/[pyruvate]	References
Normal: underwent surgery to remove tumor from posterior fossa	23–67	Microdialysis to sample extracellular fluid in posterior frontal cerebral Cx	1.7 (2.4)	2.9 (4.1)	0.17 (0.24)	23	[9][a], (Table 2)
Normal adult	22–55	^{1}H-MRS (2.1 T)/visual Cx		0.5–0.7			[10, 11]
Normal teenagers	13–16	^{13}C-MRS (2.1 T)/occipitoparietal Cx	1				[12], (Fig. 3)
Normal middle-aged adult	41 ± 13	^{1}H-MRS (4 T)/occipital lobe	1				[13][b], (Fig. 2B)
Normal young adult	19–26	^{1}H-MRS (7 T)/visual Cx	1.4	0.9–1			[14], (Fig. 3)
Normal young adult	33 ± 13	^{1}H-MRS (7 T)/visual Cx	0.62	1.01			[15], (Table 1)
Normal young adult	24 ± 1	^{13}C-MRS (4.0 T)/occipitoparietal Cx		0.75			[16][c], (Fig. 6B)
Normal young adult	25.5 (21–32)	^{1}H-MRS (2.0T)					[17], (Table 2)
		Parietal cortex					
		White matter	1.0				
		Gray matter	1.1				
		Cerebellum	1.2				
Normal young adult	20.4 ± 1.4	^{1}H-MRS (4 T)/occipital lobe		0.96			[18][d], (Table 1)
Normal elderly	76.6 ± 6.1			1.26*			
Amnesic mild cognitive impairment	Mean 85.5	^{1}H-MRS (3.0 T)/precuneus/posterior cingulate		0.16–0.99			[19][e], (Table 1)
Normal elderly	–	^{1}H-MRS (1.5 T)/occipital Cx	0.5–1				[20][f]
Probable mild-to-moderate AD	–		1.0–1.5				
			AD ↑40%*				
		^{1}H-MRS (1.5 T)/right hippocampus	Fasting Glc/Glc ingestion				[21][g], (Table 2)
Normal young adult	21 ± 3		1.42/0.97				
Normal elderly	70 ± 9		1.58/1.6				
Probable early AD	75 ± 8		1.27/2.96*				
		^{1}H-MRS (3T)/precuneus/posterior cingulate					[22][h], (Table 3)
Normal young adult	41.0 ± 10.6		0.31[h]	0.17 [h]			
Normal elderly	70.2 ± 6.7		0.36 [h]	0.17 [h]			
AD	74.3 ± 7.3		0.51 [h]*	0.20 [h]*			

Data are means, means ± SD, or ranges, and were taken from the indicated tables or estimated from the indicated figures in the cited references.

AD Alzheimer's disease, *Cx* cortex, *Glc* glucose, *MRS* magnetic resonance spectroscopy, *T* Tesla (measure of strength of magnetic field)

*$p < 0.05$. Because the brain glucose and lactate levels are influenced by metabolic rate and concentration-driven transport to/from plasma, their

Table 1 (continued)

levels in plasma are stated in the legend if they were provided

[a]Extracellular concentrations determined by intracerebral microdialysis in normal awake human brain after surgery under conditions that report about 70% of the true concentration (shown in parentheses). Pyruvate concentrations in brain are low, and are rarely determined in human brain. For comparison, lactate and pyruvate levels and lactate/pyruvate ratios in rat brain are in the range of 1.2–1.6 µmol/g, 0.09–0.12 µmol/g, and ~14, respectively, in funnel-frozen [23] and freeze-blown [24] brain. In these reports, lactate levels rose and the lactate/pyruvate ratio increased to ~50 when non-anesthetized rats were decapitated into liquid N_2 due to enhanced glycolytic metabolism during postmortem ischemia (i.e., freezing was not immediate)

[b]Brain glucose was ~1 µmol/g when plasma glucose was 5 µmol/ml, and it was ~20% of that in plasma over the range 5–30 µmol/l, in agreement with data in [12]

[c]Brain lactate level is for a plasma level of ~1.0 mmol/l, and brain level is < 2 for plasma levels up to 3 mmol/l

[d]Units of lactate are institutional units (iu) that estimate µmol/g without correction for T_2

[e]All 15 subjects had mild cognitive impairment, and represented a cohort at increased risk for transitioning to Alzheimer's disease. Lactate concentration was inversely correlated with logical memory tests, but not non-memory tasks; the higher the lactate, the lower the memory score. No controls were included in the study, but lactate levels are in the range obtained in normal subjects

[f]Characterization of probable AD was based on mini-mental state examination scores; ages of the patients were not reported

[g]Probable AD was based on low cognitive test scores that contrasted the range for normal young and elderly subjects. Metabolite levels were measured after an 8 h fast and 15 min after ingestion of 8 oz beverage containing 75 g glucose (Glc ingestion). Fasting brain glucose levels did not differ among the three groups, but the post-glucose ingestion values were significantly elevated in the probable AD group. Fasting blood glucose levels in young, elderly, and probable AD subjects were 4.2, 4.6, and 5 (*statistically significant AD vs. young and elderly), respectively, and respective post-glucose ingestion values were 6.4 (*young vs. elderly and AD), 8.8, and 7.7 µmol/l. The authors considered the reliability of brain glucose measurement poor on their 1.5 T MRS system, but values are in the range of those obtained at higher magnetic fields

[h]Values are relative to creatine

humans, but both species have similar brain/plasma ratios over the normo- to hyperglycemic range [53]. Cerebral cortical tissue and extracellular lactate levels in normal resting, awake subjects are within the range of ~0.5–3 µmol/g or ml, and the lactate/pyruvate ratio in human brain extracellular fluid is 23, similar to rat brain tissue (see Table 1 Footnote).

Levels in AD Brain In Vivo

Reduced CMR_{glc} in AD subjects is anticipated to cause brain glucose level to rise if glucose transport is not altered, and one study in probable AD patients reported a 40% rise in brain glucose level in occipital cortex [20] (Table 1). However, another study [21] found no difference in fasting brain glucose level in hippocampus of AD versus controls, whereas after glucose ingestion, brain glucose rose to a higher level in subjects with cognitive deficiency. The brain/plasma ratios for the fasted and Glc ingestion conditions, respectively, were as follows: young, 0.34 and 0.15; elderly, 0.34 and 0.18; AD, 0.25 and 0.38. The ratio in AD patients after glucose ingestion was twice that of young and elderly controls, suggesting disruption of normal homeostasis and response to a glucose challenge. A third study [22] reported that glucose levels relative to creatine in the precuneus/posterior cingulate of AD patients were ~40% and 65% higher than elderly and younger controls, respectively, whereas lactate/creatine increased by ~18% in AD. To estimate absolute concentrations, these ratios were multiplied by the creatine level reported for visual cortex in [15], 4.22 µmol/g. The respective values for glucose for young controls, old controls, and AD are 1.5, 1.5, and 2.2 µmol/g and for lactate 0.72, 0.72, and 0.84 µmol/g. The mean fasting plasma glucose level in the AD subjects was 5.0 mmol/l, so their brain/plasma ratio is ~0.44, about 50% higher than normal subjects. Patients with mild cognitive impairment had precuneus/posterior cingulate lactate levels in the normal range, but lactate level was inversely correlated with cognitive test score ([19]).

Summary

Brain glucose levels and brain-to-plasma glucose concentration ratios are relatively stable across age in normal adults and are elevated by up to about 50% in AD patients.

Concentrations of Labile Metabolites in Postmortem Human Brain

How do the levels of brain glucose, lactate, and pyruvate levels determined in postmortem samples from control subjects and patients with neurological diseases compare with values determined in living brain? To make this comparison, data from brain-bank samples that had postmortem intervals ranging from ~2 to > 45 h were tabulated for control middle-aged and elderly subjects and for patients with neurological disorders (Table 2). The results reveal substantial differences among controls and large differences in metabolite levels among subjects with the same neurological disorder. Unfortunately, some studies reported only fold-changes relative to controls, and absolute values are not available for comparison to living brain.

Table 2 Concentrations of glucose and other labile metabolites in postmortem brain of controls and subjects with degenerative brain disorders

Diagnosis	Age (years) mean ± SD (range)	PMI mean ± SD (range) (hours)	Method	Brain region	Glucose (μmol/g) or [a]fold-change relative to control	Lactate (μmol/g) or [a]fold-change relative to control	Pyruvate (nmol/g)	Ratio of [Lactate]/[pyruvate]	References
Schizophrenia	45 ± 13	34 ± 15	CE–MS	Frontal Cx		1.36[a,*]			[25][b], (Tables 2, 3)
Controls	48 ± 11	24 ± 10		Hippocampus		1.39[a,*]			
Schizophrenia	46–48	40–41	Enzymatic assays	Striatum					[26][c], (Fig. 2)
				Schiz.	1.4	1100*	0.58*	1.9×10^6	
MRDS	46–48	42–44		MRDS	1.1	1100*	0.48	2.3×10^6	
nMRDS	45–47	38–39		nMRDS	1.7*	1200	0.6*	2×10^6	
Controls	47–50	41–45		Cont.	1.3	900	0.4	2.3×10^6	
HD	65 (57–73)	11.2 (9–13)	GC–MS	Putamen					[27][d], (Table 2)
				Fructose	5.2[a,*]				
				Sorbitol	3.6[a,*]				
				Glucose	8.4[a,*]				
Controls	67 (60–75)	10.6 (8–13)		Glc-6-P	13.1[a,*]				
AD	70.3 ± 7.1	7 (4–12)	GC–MS	7 regions		0.5–7.3[a] but significant rise only in hippocampus (2.6[a,*])			[28, 29][e]
				Fructose	3.9–5.7[a,*]				
				Sorbitol	3.0–4.3[a,*]				
				Glucose	5.2–16.4[a,*]				
Controls	70.1 ± 6.7	9 (5.5–13)		Glc-6-P	3.8–8.5[a,*]				
AD	87.9 ± 8.9	14.7 (3–23)	Flow-injection MS	MFG	785* (1.3[a])				[5][f], (Fig. 2A)
AsymAD	89.2 ± 7.9	14.8 (2–33)			722* (1.2[a])				
Control	82.6 ± 11.0	16.9 (7–28)			611				
AD				ITG	853* (1.8[a])				
AsymAD					611* (1.3[a])				
Control					476				
AD				Cerebellum	517 (1.4[a])				
AsymAD					289 (0.8[a])				
Control					372				
AD	85.7 ± 6.9	44.3 ± 22.8	^{1}H MRS	Brodmann 7 region, neocortex		10.9			[30][g], (Table 4)
Controls	77.9 ± 11.7	45.3 ± 26.9				9.9			

Metabolite levels were determined in extracts of postmortem tissue, and values are means ± SD, means (ranges), or ranges. Data from cited references were taken from the indicated tables or estimated from the indicated figures.

AD Alzheimer's disease, *AsymAD* asymptomatic AD, *CB* cerebellum; *CE-MS* capillary electrophoresis-mass spectrometry, *Cx* cortex, *Glc-6-P* glucose-6-phosphate, *GC–MS* gas chromatography–mass spectrometry, *HD* Huntington's disease, *ITG* inferior temporal gyrus, *MFG* middle frontal gyrus, *MRDS* cortical muscarinic receptor-deficient schizophrenia, *nMRDS* non-muscarinic receptor-deficient schizophrenia, *MRS* magnetic resonance spectroscopy, *PMI* postmortem interval (time from death to tissue freezing), *schiz* schizophrenia

*$p < 0.05$ versus control. Note that investigators made strong efforts to match PMI, age, and gender for controls and disease states

[a]Fold-change relative to control for statistically significant differences from controls

[b]Values are acquired peak area divided by that of internal standard and sample volume, then normalized to controls as fold-change

[c]Cadavers were refrigerated within 5 h after death and frozen at −70 °C within 30 min of autopsy. Demographic data varied among the subjects used for different metabolite assays, and ranges of means for the different groups are tabulated. Metabolite levels were reported for the control and overall schizophrenia groups and also schizophrenia subgroups with MRDS or nMRDS. Lactate/pyruvate ratios were calculated from the mean reported levels. Note the extremely high lactate levels and lactate/pyruvate ratios and very low pyruvate levels (compare to Table 1)

[d]HD/control from putamen, a highly-affected brain structure in Huntington's disease (HD). This study also reported the fold-change in abundance of 63 metabolites in 11 brain regions

[e]Ranges of AD/control for glucose, sorbitol, and fructose in seven brain regions are from Table 3 of [28]. Glc-6-P and lactate are from Table 2 of [29] that provided a more detailed report of the fold-changes for 55 metabolites that were altered in more than one AD brain region

[f]Glucose levels are for three brain regions (ITG, MFG, and cerebellum) from controls, AD, and AsymAD (asymptomatic AD patients who had significant AD neuropathology at autopsy without cognitive impairment). Tabulated fold-changes relative to control for each region indicated in parentheses were calculated from the mean values

[g]Among the other metabolites measured, alanine level increased significantly from 0.65 to 0.75 μmol/g in controls and AD, respectively, whereas glycine (0.38 and 0.38 μmol/g) and serine (0.42 and 0.45 μmol/g) levels did not change in the respective groups. Note that these amino acid concentrations at long PMIs differ somewhat from those in the epileptic focus of cerebral and cerebellar tissue in Table 3B with shorter PMIs

Table 3 Postmortem changes in brain concentrations of glucose and selected amino acid levels

A. Glucose	References	Species	Brain region	Initial concentration (μmol/g)	Percent of initial concentration at intervals after death[a]								
					4 s	6 s	10 s	15 s	30 s	1 min	2 min	5 min	30 min
	[31][b], (Fig. 1, Table 3)	Mouse	Whole brain	1.5	82	67	53	33	11	11	11		
	[32] [c], (Table 1)	Rat	Cerebral cortex	2.65									5.3
	[33] [d], (Figs. 1, 2; Table 1)	Dog (anesthesia)	Cerebral cortex	3.17					53	43	16	0	
	[34][e], (Fig. 1; Tables 1, 3, 4)	Human (anesthesia)	Parietal cortex	5.8					87	78	59	37	0
			White matter	6.3									
			Frontal lobe										
			Gray matter	3.1								10	3
			White matter	2.1								38	10
	[35][f], (Table 1)	Mouse	Whole brain	0 h	12 h	24 h	36 h	48 h	60 h				
				0.28	257	357	678	1821	2286				

B. Amino acids	References	Species	Brain region	Initial concentration (μmol/g)	Percent of initial concentration at intervals after death[g]						
					2 min	30 min	1 h	2 h	4 h	24 h	48 h
	[36] [h], (Tables 1, 2)										
Serine		Rat	Whole brain	0.84	105	108	99	112	127	157	225
Glycine				1.06	101	106	124	120	137	200	252
Alanine				0.42	121	171	200	221	231	317	360
		Human (anesthesia)	Cerebral and cerebellar cortex (epileptic focus)		10 min	30 min	1 h	2 h	4 h		
Serine				0.49	107	111	117	144	168		
Glycine				0.85	91	113	155	194	208		
Alanine				0.49	108	157	230	290	396		

Examples of glucose (Glc) concentration measured (i) in extracts of brain using procedures to quickly inactivate brain enzymes and minimize or prevent loss of labile metabolites and (ii) after their rapid consumption by increased postmortem metabolism due to ischemia. Data are from the indicated tables and figures in the cited references

[a]Percent of initial concentration at intervals after death was calculated as 100 × (concentration at time = t)/(concentration at time = 0)

[b]Awake adult mice were decapitated and their heads were either immediately frozen in Freon 12 at − 150 °C with stirring or maintained at 38 °C until frozen at timed intervals. At 10 min after decapitation, ATP and phospho(P)-creatine (PCr) levels were near zero, Glc-6-P and fructose-1,6-P_2 were ~ 15–25% of zero time, and lactate level increased > 10-fold from an initial value of ~ 1 μmol/g

[c]Unanesthetized rats were subjected to 30 min of forebrain ischemia and their brains were frozen in situ with liquid nitrogen while they were unconscious. At this time, PCr and ATP levels were 1–2% of those in operated controls

[d]Brains of amytal-anesthetized dogs were obtained by in situ freezing or were decapitated and brain samples were frozen at timed intervals

Table 3 (continued)

[e]Samples of normal parietal and frontal cortical gray and white matter that had to be removed to gain access to brain tumors were very carefully excised from human brain during surgery under general anesthesia, samples were frozen in Freon 12 at − 150 °C within a few seconds after excision, and separate portions were anaerobically incubated under mineral oil for timed intervals at 37 °C, then frozen. Note that metabolic rates are lower under anesthesia than in the awake or unanesthetized state due to reduced neural activity and energy demand, and energy metabolites are depleted at a slower rate [31]

[f]Albino mice were euthanized under ether anesthesia, left at 22 °C until organs were excised, then stored at − 50 °C until analyzed. Glucose levels reported as mg/g tissue protein were converted to µmol/g brain by multiplying by 0.555, assuming 0.1 g protein/g brain. The postmortem interval at between death and tissue homogenization for the 0 h samples was not stated, and the 0 h values are very low (20% of initial values in [31]) because no precautions were taken to preserve labile metabolites after death and during homogenization of tissue in ice-cold PBS solution. The low zero time value inflated the percent changes with time after death

[g]Values for amino acid concentrations in rat and human brain at intervals after death are expressed as percent of the respective zero time values as tabulated in reference [36]

[h]Concentrations of amino acids in postmortem rat and human brain were selected from more detailed data sets of 35 amino acids and related compounds. Rats were decapitated, brains quickly removed, and frozen in liquid nitrogen within 30 s after death or at timed intervals up to 48 h thereafter. Biopsies of human brain were obtained from anesthetized patients during surgery to remove an epileptic focus; portions of the samples were frozen in liquid nitrogen immediately or after timed intervals up to 4 h

Take Home Message

Postmortem brain glucose, lactate, and pyruvate levels reported for control, Huntington's disease, or AD subjects do not correspond to their respective concentrations in living brain determined by ^{1}H-MRS or microdialysis. Discrepant glucose levels were obtained in different studies in AD brain: extremely low values probably arose from postmortem ischemia, whereas unrealistically-high values are not explained. An important issue is that fold-changes and plots of glucose levels expressed as $\log_2$[glucose] or ln[glucose] obscure the actual concentrations and make it difficult for readers and reviewers to assess data validity.

Schizophrenia

Postmortem glucose levels in control and schizophrenic brain were close to the normal range in vivo (compare Tables 1, 2), and only non-muscarinic receptor-deficient schizophrenia (nMRDS) had levels significantly above control. Strikingly, however, all postmortem lactate levels exceeded that in normal brain by ~ 1000-fold, whereas pyruvate levels were considerably lower and lactate/pyruvate ratios were ~ 5 orders of magnitude higher than in normal interstitial fluid (compare Tables 1, 2). In normal brain, postmortem lactate levels are about twice the sum of brain glucose plus glycogen levels at death [31, 33, 34], i.e., two lactate are produced from each glucosyl moiety under anoxic conditions. However, glucose + glycogen levels in normal brain are much too low to account for the extremely high lactate levels and the extraordinarily-elevated lactate/pyruvate ratios ([26], Table 2), raising the question of whether the reported lactate levels or their units of concentration are correct (Box 1).

Huntington's and Alzheimer's Diseases

Large data sets of regional fold-changes in metabolite levels relative to controls were reported for Huntington's disease brain [27] and AD [28]. An abbreviated tabulation of these data is shown in Table 2 that lists only the *ranges* of fold-increases above controls for the putamen in Huntington's disease and for seven brain regions in AD. In both Huntington's disease and AD, the relative fold-increases in levels of glucose and two metabolites in the polyol pathway, sorbitol and fructose, ranged from ~ 3.6 to 16, depending on brain region and disease. A 5–16-fold higher range for brain glucose concentration in Huntington's disease and AD subjects relative to age- and postmortem interval-matched controls is remarkably high, and based on normal brain glucose level (~ 1 µmol/g, Table 1), the brain glucose level would be 5–16 µmol/g. Lactate level was also elevated in all AD brain regions, but was statistically significant only

Table 4 Calculated estimates of glycolytic rate and indirect evaluation of net glycolytic enzyme activities in postmortem human brain: (A) postmortem glycolytic rates in human surgical samples and indirect activities calculated from human brain glucose and amino acid levels, (B): indirect glycolytic enzyme activities in control, asymptomatic AD and AD brain

References	Subject	Region	PMI	CMR_{glc} (μmol/g/min)	Triose flux (μmol/g/min)	Estimated HK–PFK activity[b] [Ser + Gly]/[Glc] (no units)	Estimated PK activity[b] [Ser + Gly + Ala]/[Glc] (no units)
A. [34][a]	Brain tumors excised under anesthesia	Normal parietal Cx gray matter	~0 min	0.26	0.52	0.23[b]	0.32[b]
			Peak ischemia	3.4–3.8 [c]	6.8–7.6		
			0–5 min interval	1.3 [d]	2.6		
			1 min			0.30[b]	0.40[b]
			5 min			0.62[b]	0.85[b]
			30 min			∞[b]	∞[b]
B. [5][e]	Control	ITG	~15–17 h			6.0	10.3
	AsymAD					3.7	7.4
	AD					2.7*	4.6*
	Control	MFG				3.7	5
	AsymAD					2	4
	AD					2	4
	Control	Cerebellum				8.7	15
	AsymAD					8.7	15
	AD					4	8

AD Alzheimer's disease, *AsymAD* asymptomatic AD, *MFG* middle frontal gyrus, *ITG* inferior temporal gyrus

[a]Samples of normal parietal and frontal cortical (Cx) gray and white matter that had to be removed to gain access to brain tumors were very carefully excised from human brain during surgery under general anesthesia, samples were frozen in Freon 12 at −150 °C within a few seconds after excision [34]. Separate portions of these samples were anaerobically incubated under mineral oil for timed intervals at 37 °C, then frozen; data are from Fig. 1 and Tables I, II, and III of [34]. The resting in vivo rate of glucose utilization (CMR_{glc}) was estimated by Kirsch and Leitner [34] according to the procedure of Lowry et al. [31]. CMR_{glc} denotes the rate of glucose utilization at the hexokinase step, and the rates of triose and tricarboxylic acid cycle fluxes are twice CMR_{glc} because two trioses (and 2 pyruvate) are produced per glucose molecule

[b]Estimates of hexokinase plus phosphofructokinase (HK + PFK) and pyruvate kinase (PK) activities were calculated as the ratios of concentrations of amino acids to glucose (see text) using (i) the initial parietal cortex glucose level and the amount of glucose remaining at various times shown in Table 3A, and (ii) the respective human amino acid concentrations in Table 3B, with the assumption that their levels were stable at 1 and 5 min after death, since changes at 10 min were < 10%

[c]The estimated peak rates during the first 30 s of ischemia in parietal cortex were calculated as either the amount of glucose plus glycogen consumed or as the amount of lactate formed in the representative example in Fig. 1 of Kirsch and Leitner [34]

[d]The overall mean estimated CMR_{glc} over the 0–5 min interval was calculated from the net change in hexose concentration in Table II of Kirsch and Leitner [34]

[e]Mean values for HK + PFK and PK were estimated from Figs. 2B and 2C of [5]

in hippocampus. In contrast, brain lactate levels in the Brodmann 7 region of neocortex did not differ in control and AD samples that had relatively long postmortem intervals (Table 2), and both levels were ~10 μmol/g (10 times normal), a reasonable value for postmortem brain. The large relative increases in glucose, sorbitol, and fructose levels were interpreted by the authors [27–29] as reflecting ante mortem hyperglycemia/diabetes in Huntington's disease and AD, such that increased flux into the polyol pathway to produce the sorbitol may contribute to neurodegenerative outcomes.

How do these putative hyperglycemic brain levels in Huntington's disease and AD brain compare to the literature? A summary of diabetes-related studies showed that the mean plasma glucose in rodent animal models increased from ~9 to 27 mmol/l and mean brain glucose level rose from ~2 to 7 μmol/g, whereas in diabetic humans, arterial plasma glucose approximately doubled from 6 to 8 to 14 mmol/l and brain glucose relative to creatine rose ~1.5-fold [54]. High glucose levels increase its flux into the polyol pathway, cause oxidative stress, and contribute to complications of diabetes [55, 56], but the relative increases in postmortem Huntington's disease and AD brain appear to exceed the levels in human diabetics by a large margin.

Because cadaver tissue from demented diabetic patients was not available, Xu et al. [28] measured metabolite levels in streptozotocin-induced hyperglycemic rats (a model for diabetes) and a triple-transgenic mouse model for AD.

Absolute values were not stated, but 5.3-, 5.8-, and 4.6-fold increases in glucose, sorbitol, and fructose, respectively, were reported for streptozotocin-treated rats. Their AD-model mouse brain glucose levels were below their limit of detection (~ 1–5 µmol/kg or ~ 1–5 nmol/g). Unfortunately, the tissue harvesting/processing procedures used by Xu et al. [28] have technical shortcomings that caused losses of labile metabolites and invalidated their conclusions. The rats and mice were euthanized with isofluorane, which alters the levels of many brain metabolites, including reducing glucose and increasing lactate [57]. Rat brains were excised and snap frozen within ~ 1 min, which is too slow to preserve all glucose (see below, Table 3), although the residual glucose in hyperglycemic streptozotocin-treated rats may still exceed control. Euthanized mice were transcardially perfused with 0.9% NaCl, brains removed, and snap frozen. Glucose would be consumed before and during the perfusion, explaining its undetectable levels. These animal studies do not support results in Huntington's disease and AD brain, and, in fact, they are consistent with the rapid postmortem metabolism of glucose that would eliminate glucose from brain-bank samples.

Two critical questions remain (Box 1): What are the absolute values for the controls and AD patients? How do they compare to in vivo MRS measurements? Two sets of data included in Table 2 reported increased glucose levels in AD brain, but closer examination of the data and conversion from reported units that were expressed as logarithms of the concentrations to standard units of concentration, µmol/g reveals discrepant findings.

Extremely Low Glucose Levels in Postmortem AD, Huntington's and Control Brains

Actual concentrations, not fold-changes, are required to determine whether hyperglycemia exists in Huntington's disease and AD brain. Figure 1 of Xu et al. [28] did report regional glucose levels that were expressed as $\log_2$[glucose], but the authors did not state the units of concentration in their table/figure legends or Methods. Almost all of their $\log_2$[glucose] for controls were less than -6, the antilog of which is <0.015. Most $\log_2$[glucose] values for AD subjects ranged from -6 to -2, equivalent to a range of 0.015–0.25. The fasting plasma glucose levels for AD and controls were stated to be essentially the same, 5.0 and 5.1 mmol/l, respectively (Suppl. Table S2 in [28]). If the brain/plasma ratio for the AD subjects were assumed to be elevated to 0.5 (higher than values in the living brain, see discussion of data in Table 1, above), the brain glucose level may be approximately 2.5 µmol/g for Huntington's disease and AD brain, compared to brain/plasma ratio of 0.3 for controls and an estimated 1.5 µmol/g brain glucose. These values yield a 67% rise in brain glucose level in AD, not a 5–16-fold increases as inferred from fold-changes in Huntington's disease and AD patients [27–29].

A useful approach to quickly identify unrealistic measured brain levels is to (i) compare the concentrations to those in living brain, preferably determined by a different method, and (ii) multiply the arterial plasma concentration by the brain/plasma distribution ratio for normal and diseased brain to obtain an estimate of the anticipated brain glucose concentration (Box 1). Outliers can be then quickly recognized and re-evaluated to establish or rule out validity.

Regardless of glucose concentration units (e.g., µmol/g, mg/g tissue, or mg/mg protein), these values are about 1/10th to 1/100th of in vivo values (see Table 1), as expected for glucose-depleted postmortem tissue. These data may represent residual glucose remaining after postischemic energy failure, differences in Huntington's disease and AD brain composition (e.g., glycolipid or glycoprotein), and/or (regional) variations in autolytic activity that may be relevant to neurodegenerative diseases. Given the long postmortem intervals for both matched controls and AD subjects (4–13 h) and extremely low postmortem glucose levels, severe hyperglycemia/diabetes in brain of living AD and Huntington's disease subjects was not established and is considered to be very unlikely.

The companion paper by Xu et al. [29] provided a more detailed report of the fold-changes for 55 metabolites that were altered in more than one AD brain region, including glucose-6-phosphate (Glc-6-P) and lactate. However, these values are also suspect because Glc-6-P is depleted and lactate levels rise when postmortem tissue freezing is not immediate, as has been shown for rats that were decapitated into liquid nitrogen [23, 24]. Based on group/subject descriptions in Tables 1 and 2 and Supplementary Table 1 in [28, 29], the same patient population was used. However, both the ranges and fold-changes reported for glucose, fructose, and sorbitol in the seven brain regions in Table 3 of [28] are not the same as in Table 2 of [29], raising uncertainty of the actual fold-changes. Unfortunately, absolute values for the additional metabolites reported (besides glucose) were not provided by Xu et al [29]. The impact of postmortem autolytic changes cannot, therefore, be evaluated to validate potential disturbances in respective metabolic pathways to be targeted in future studies.

Extremely High Glucose Levels in Postmortem AD and Control Brain

In contrast to the extremely low glucose levels discussed above, another study using postmortem AD brain reported impossibly-high glucose concentrations in three regions of control and AD brain. Why weren't these data recognized as unreasonable by the authors, reviewers, and editors? One possibility is that numerical data were ambiguous because they

were expressed as logarithmic values and 'quick checks' to evaluate the validity of the data (Box 1) were not carried out.

The featured article by An et al. [5] that was highlighted [58] reported postmortem (postmortem interval range: 2–33 h) glucose levels in three brain regions from controls, AD, and asymptomatic AD (AD patients who had significant AD neuropathology at autopsy but no cognitive impairment). The middle frontal gyrus and inferior temporal gyrus were stated to be vulnerable to amyloid and tau deposition, respectively, whereas cerebellum is resistant to classical AD pathology. Brain glucose levels were higher than control in the middle frontal gyrus and inferior temporal gyrus in AD and asymptomatic AD tissue, but not in cerebellum, linking changes to regions vulnerable to AD (Table 2). Note that the AD/control fold-changes (1.2–1.8) were much smaller than those of Xu et al. [28, 29] (Table 2).

The glucose levels reported by An et al. [5] in their Fig. 2A were expressed as the natural logarithm of [glucose], with units of nmol/mg tissue. For their tabulation in Table 2, estimates of the mean values were converted to µmol/g by taking the antilogs of ln[glucose]. The 'glucose' determined by flow injection-mass spectrometry was stated to include all hexoses in brain extracts, and hexose was assigned to glucose based on its high concentration in blood and brain compared with other hexoses. However, all of the 'glucose' levels were extraordinarily high, ranging from about 370–850 µmol/g, exceeding those in normal living brain by ~300–800-fold. These values cannot represent the small metabolic pool that is consumed shortly after death.

Three easy checks could have identified potential problems with these data (Box 1). First, compare the concentrations to in vivo MRS data. Second, calculate the anticipated brain glucose level from that in plasma, as discussed above. The average plasma glucose levels in all groups during follow-up and measured during the 2.7–8.8 years prior to death was about 5.5 mmol/l (Table 4 of [5]). The anticipated estimates of brain glucose concentrations calculated with brain/plasma distribution ratios of 0.3 for control and 0.5 for AD subjects are 1.7 and 2.8 µmol/g, respectively. These estimates are well below the reported values (Table 2). Third, influx of glucose and [^{18}F]FDG from blood to brain is equilibrative, and these high brain levels, if true and apply to all AD patients, would cause glucose *efflux* down its concentration gradient from brain to blood. This implies active transport to get such high levels of glucose into the AD and control brain, which has never been demonstrated. High brain glucose levels would compete with tracer levels of [^{18}F]FDG for its uptake and phosphorylation in PET assays to cause very low apparent CMR_{glc} in *all brain regions* of AD and control cohorts. However, low CMR_{glc} in AD brain is selective to vulnerable regions, arguing against extremely high glucose levels throughout AD (and control) brain. Thus, simple, straight-forward tests of data validity (Box 1) could have raised a red flag and stimulated re-analysis of the questionable data.

Summary

The methods used to assay metabolite levels in human brain are limited. Brain microdialysis has been very important for real-time bedside monitoring of brain status to guide neurocritical care during and after surgical intervention [59]. MRS can be used in control subjects and patients with neurological disease who can tolerate being in the scanner. MRS has many technological advantages, but the equipment is expensive and requires technical support and a critical mass of scientists. Surgical samples of human brain have been obtained and used to determine levels of amino acid and glycolytic metabolites, with the requirement for immediate freezing to stop metabolism [34, 36, 60–62] (see below, Tables 3, 4). The studies in postmortem brain utilized rigorous analytical procedures, but they were compromised by rapid metabolism of glucose and other labile metabolites upon death. Quick check procedures (Box 1) can help identify unreasonable data and outliers.

Rates and Magnitudes of Postmortem Changes in Glucose and Amino Acid Levels

Blood flow to the brain ceases at death, stopping delivery of glucose and oxygen (i.e., ischemia) and removal of lactate, so glucose and glycogen are depleted, and lactate level rises (Box 1). The preceding discussion alluded to loss of labile metabolites in postmortem brain, but did not provide information about how fast this occurs or the magnitude of change.

Take-Home Message

Depletion of PCr, ATP, glucose, and glycogen by ischemia halts glycolytic metabolism. Glucose levels detected at postmortem intervals > 30 min are inflated, presumably by autolysis. Postmortem concentration changes for most amino acids are slower than those of labile energy metabolites, and most progressively rise with time. Each compound of interest has its own trajectory of concentration change after death, and temporal profiles must be established in brain regions and diseases of interest in tissue from controls and patients to properly interpret findings in postmortem tissue (Box 1).

Rapid Glycolytic Upregulation Consumes Labile Metabolites

Comprehensive analysis of the time courses of postmortem changes in energy metabolite levels in adult mice in the classic

study by Lowry et al. [31] revealed a peak sevenfold initial increase in glycolytic rate immediately after death. Half of the baseline glucose was gone within 10 s, 90% was consumed at 2 min (Table 3A), and it was virtually gone by 10 min. In rats with forebrain ischemia, 95% of the glucose was metabolized within 30 min. Anesthesia reduces neural activity, energy demand, and metabolic rates, and it slowed glucose clearance from anesthetized dog brain, but it was still gone by 5 min. Similarly, when surgical explants of normal anesthetized human brain were frozen immediately and at timed intervals after anaerobic incubation at 37 °C, some glucose could be detected in gray matter at 10 min, but it was depleted by 30 min. White matter has a lower CMR_{glc} [63], and glucose clearance was also slower than in gray matter. PCr and ATP were quickly consumed in human ischemic gray and white matter and in glioblastoma samples [34, 61], as occurs in mice [31]. Together, these findings in four species demonstrate that the metabolic pool of glucose and the energy reserves in glycogen, ATP, and PCr are depleted within a few minutes of ischemia and are essentially completely consumed by 30 min after death.

Progressive Postmortem Increases in Brain Glucose Level

A study with mice that did not use precautions to prevent postmortem loss of labile metabolites ([35], Table 3A) had a very low initial brain glucose concentration (0.28 µmol/g) that progressively increased by 2.6-fold (0.71 µmol/g) at 12 h and by 23-fold (6.4 µmol/g) at 60 h in cadavers stored at 22 °C. The progressive increase in glucose concentration in postmortem tissue presumably arose from autolysis of endogenous glucose-containing compounds (e.g., glycolipids and glycoproteins) because the above studies show that glucose is reduced by > 90% within 30 min of ischemia. (Note that the values in Table 3 are expressed as percent of the zero time value, whereas fold-change represents the ratio of concentration at time = t divided by that at time = 0).

Postmortem Changes in Amino Acid Levels

Levels of 35 amino acids and related compounds also change heterogeneously and substantially with time after death in both rat and human brain, but most alterations are slower than for energy metabolites [36]. However, two exceptions are alanine and GABA. Alanine level falls within seconds after decapitation, and after a lag of about 1 min, the concentrations of alanine and GABA rise rapidly for a few min, followed by slower, steady increases during the ensuing 30 min [8]. Some amino acid levels are unchanged for long periods of time, whereas many others progressively increase by two–seven-fold at 4 h in human brain, with some rising by 11–50 fold at 48 h in rat brain (not shown, see [36]), presumably due to postmortem hydrolysis of proteins and peptides.

Attention is directed to 1.7–4-fold increases in the levels of serine (Ser), glycine (Gly), and alanine (Ala) in human brain at 4 h after death, and similar increases in rat brain up to 48 h (Table 3B). The levels of these amino acids were used by An et al. [5] in a novel approach to evaluate glycolytic activity in postmortem human brain (see below).

Summary

Labile energy metabolites in the glycogen, glycolytic, and oxidative pathways are quickly depleted when blood flow to the brain ceases. Most amino acid concentrations are not stable after death and they change more slowly than energy metabolites. Each compound has its own trajectory of postmortem change, and percent changes are highest for compounds with the lowest initial concentration.

In Vitro Metabolic Assays in Freshly-Excised and Postmortem Human AD Brain Tissue

If availability of energy metabolites is exhausted within minutes after death, are there other approaches to use postmortem tissue to extract information about metabolic capability in diseased compared with control brain tissue? One possibility is to use brain slices or homogenates if the postmortem interval is short and enzymes activities are stable. Rodent brain slices are commonly used for many studies, ranging from metabolism to electrophysiology.

Take-Home Message

Postmortem tissue is suboptimal for metabolic assays compared with freshly-excised tissue. Reduced glucose utilization in vivo is not reflected by altered conversion of [U-^{14}C]glucose to $^{14}CO_2$ in fresh tissue samples in vitro. In fact, glucose oxidation in AD brain tissue prisms was higher than control, whereas it was subnormal in homogenates of frozen, postmortem tissue. In vitro rates are substantially less than glucose oxidation rate in vivo.

Brain Tissue Slices

A series of studies by Sims et al. [64–67] used samples of frontal and temporal lobe cortical gray matter that was excised by diagnostic craniotomy to confirm Alzheimer's disease or taken from apparently-normal control cortex of patients to allow surgical removal of tumors. AD was confirmed by histopathology of adjacent tissue samples that revealed senile plaques

and neurofibrillary degeneration. Tissue was cut into prisms within 2 min after excision and incubated with [U-^{14}C]glucose and assayed for $^{14}CO_2$ production, [^{14}C]acetylcholine synthesis, incorporation of ^{14}C into amino acids, and ATP concentrations. Even with a 30 min postmortem interval at 37 °C, synthesis of [^{14}C]acetylcholine in the presence of 31 mmol/l K^+ to depolarize the cells was substantially reduced. In contrast, at 5 mmol/L K^+, a longer duration (up to 2 h) was required to impair $^{14}CO_2$ production and [^{14}C]acetylcholine synthesis. Notably, there was no correlation of rates of $^{14}CO_2$ production and [^{14}C]acetylcholine synthesis in fresh tissue samples across age from about 15 to 68 years. [^{14}C]Acetylcholine synthesis in AD brain was reduced to 47% of control, presumably reflecting loss of cholinergic nerve endings. $^{14}CO_2$ production in samples of temporal and frontal cortex from AD patients was elevated above control by about 25–40%. Calculated rates of $^{14}CO_2$ production (after conversion from reported values of dpm/mg protein/min, assuming 100 mg protein/g brain) for all samples in 5 and 31 mmol/l K^+, respectively, were 0.39 and 1.05 nmol/g/min for controls and 0.55 and 1.35 nmol/g/min for AD brain prisms. For comparison, resting CMR_{glc} in normal human adult brain in vivo is ~ 0.3 µmol/g/min [68], equivalent to 1.8 µmol CO_2/g/min when all glucose is oxidized ($6O_2 + 1$glucose $\rightarrow 6CO_2 + 6H_2O$). Incorporation of ^{14}C into the total amino acid pool (dpm/nmol) was not altered in AD, although there was a small decrease in total amino acid concentration. ATP and AMP but not ADP concentrations were reduced 20–30% in samples from AD patients.

Brain Homogenates

As a follow up to earlier FDG-PET reports of reduced CMR_{glc} in AD patients, Swerdlow et al. [69] evaluated glucose oxidation in postmortem temporal cortex from age-matched controls and AD subjects (postmortem interval = 12–18 h at which time samples were frozen at − 70 °C). $^{14}CO_2$ production by homogenates incubated with [U-^{14}C] glucose was highest, ~ 6 pmol CO_2/g/min, in young controls (mean age, 31.8 years) and declined with age: the rate in normal elderly was 53% of that in young adults (73.8 years), and it was even lower, only 13%, in AD patients (73.2 years).

Summary

These contrasting data sets in fresh tissue prisms and homogenates reveal limitations of metabolic assays in fresh versus frozen postmortem tissue compared with living brain. Glucose oxidation rates in tissue prisms with intact cellular structure were about three orders of magnitude higher than in homogenates (due, in part, to cellular destruction and elimination of ionic gradients) and three orders of magnitude lower than in vivo (due to deafferentation, postischemic recovery, and other factors).

Indirect Evaluation of Hexokinase (HK)–Phosphofructokinase (PFK) and Pyruvate Kinase (PK) Activities

The postmortem concentrations of glucose and three amino acids derived from trioses in the glycolytic pathway (see Fig. 1a: serine, Ser; glycine, Gly; and alanine, Ala) were used to calculate activities of key glycolytic enzymes as follows: HK + PFK = ([Ser] + [Gly])/[Glc] and PK = ([Ser] + [Gly] + [Ala])/[Glc]. These ratios were stated by An et al. [5] to represent the net hexose activities of HK + PFK and net triose activity of PK. These ratios are dimensionless because concentration units cancel out, and they are not metabolic rates or enzyme activities (i.e., µmol/min/g tissue or mg protein). All three amino acids are derived from trioses downstream of the aldolase reaction that converts fructose-1,6-P_2 to two trioses (Fig. 1a), and the calculations infer that amino acid concentrations are related to the upstream enzyme activities. However, the true rates for triose flux would be twice those of HK–PFK flux, since two trioses are formed from each hexose. It is not clear that inclusion of alanine concentration in the PK calculation can register a twofold increase above HK + PFK since the sum of alanine + serine + glycine concentrations is only 22–37% higher than the sum of serine + glycine concentrations in rat and human brain (Table 3B).

Take Home Message

An alternative approach to evaluate glucose utilization is to calculate pathway fluxes based on measured concentrations of their components. An et al. [5] devised a novel, indirect approach to calculate glycolytic activity from metabolite levels determined in postmortem AD brain, but they *did not test and validate* their method to prove that their calculated values and the actual enzyme activities are equivalent. Two initial checks of their method reveal that postmortem ischemia and autolytic changes drive the calculated enzyme activities that do not represent the vivo fluxes of labeled glucose into metabolites.

Influence of Postmortem Metabolite Concentration Changes

An obvious initial concern is that the levels of glucose, serine, glycine, and alanine are not stable in postmortem brain (Table 3), and their use to estimate glycolytic enzyme activities may give misleading results that vary with postmortem interval. Postmortem increases in [Ala] were most rapid in both rat and human brain, followed by slower and smaller increases in [Gly], with a longer lag for [Ser]; all three increased ~ 1.7–4-fold at 4 h in human brain (Table 3B).

Due to rapid postmortem elimination of glucose (Table 3A), glycogen, PCr, and ATP metabolic pools, net glycolytic flux is near zero by 30 min after death. These findings indicate that calculated postmortem activities of glycolytic enzymes using the above equations of An et al. [5] will be initially and briefly driven upward by rapid decreases in glucose concentration, accompanied shortly later by the rise in [Ala], and more slowly by shifts in [Ser] and [Gly], presumably due to metabolic responses to ischemia, then autolytic and proteolytic activity (Box 1).

Labeling of Lactate and Amino Acids by Glucose

If calculated HK + PFK and PK activities represent the respective hexose and triose fluxes, labeling of the amino acids used in the calculations might be anticipated to reflect the flow of glucose carbon through the glycolytic pathway. This possibility was assessed by metabolic labeling of lactate and amino acids by [U-^{14}C]glucose in rat brain [8]. [^{14}C] Glucose quickly entered the brain after the pulse intravenous injection, its concentration peaked within 1 min, and it was rapidly metabolized, causing its concentration to fall with time (Fig. 1b). Of the identified metabolites, the initial rate and magnitude of labeling of lactate was highest, followed by glutamate (Fig. 1b) that is labeled via the TCA cycle (Fig. 1a). Glutamate continued to accumulate label for 15 min due to dilution of the ^{14}C in the large, unlabeled glutamate pool. After an initial lag, labeling of other TCA cycle-derived amino acids (glutamine, aspartate, GABA) exceeded that of alanine and was much greater than those of serine and glycine; glycine labeling was delayed by > 30 min and was very low thereafter. Of note, alanine and lactate are both derived from pyruvate (Fig. 1a), yet their labeling differed considerably (Fig. 1b). This means that the flow of ^{14}C tracer label from glucose traverses the glycolytic pathway to pyruvate/lactate without equivalent labeling of alanine, serine, and glycine (Fig. 1a). From pyruvate, label quickly enters the TCA cycle and is incorporated into glutamate and other amino acids faster than into serine, glycine, and alanine. Thus, glucose-derived ^{14}C flux from pyruvate to lactate greatly surpassed the rates of *lateral* label incorporation into alanine and the *upstream* label incorporation from 3-phosphoglycerate into serine and of label from serine into glycine (Fig. 1a, b). Dynamic labeling of the amino acids derived from glycolysis does not report glycolytic flux, and it is unlikely that their *concentrations relative to glucose* are relevant to or predictive of rate-limiting enzyme activities. This is a concern because animal studies of brain activation reveal that brain glucose concentration can be constant even as glucose utilization increases because glucose supply matches demand; glucose concentration per se does not report metabolic rate [70].

Summary

There are two reasons to question the validity of the calculations to estimate activities of HK + PFK and PK [5]: (i) the calculated values are governed by time-dependent postmortem changes in concentrations of glucose and amino acids. (ii) Flux of label from glucose into lactate and the TCA cycle is not reflected by labeling of serine, glycine, and alanine.

Tests of the Indirect Method to Evaluate In Vivo Glycolytic Enzyme Activities

To my knowledge, there are no complete data sets with measurements of glycolytic rate and amino acid concentrations to test directly the validity of the calculated glycolytic enzyme activities. Three alternative approaches were, therefore, used to evaluate the method: (i) compare glycolytic rates during very short ischemic intervals with those based on glucose and amino acid concentrations. (ii) Compare amino acid levels calculated from reported glucose levels and calculated indirect enzyme activities with postmortem levels in human brain. (iii) Compare indirect calculated activities with HK, PFK, and PK activities measured in vitro.

Take-Home Message

The theoretical calculations to estimate glycolytic enzyme activities do not agree with values determined from changes in metabolite concentrations measured during the immediate postischemic interval, the amino acid levels calculated from reported postmortem glucose levels and enzyme activities are unrealistically high, and calculated enzyme activities do not correspond to measured activities in vitro. The method is not validated.

Glycolytic Rates in Surgical Samples from Human Brain Versus Indirect Calculated Rates

To evaluate the use of [amino acid]/[glucose] ratios to indirectly evaluate glycolysis in human brain, calculated ratios representing HK + PFK and PK activities were compared to rates determined in quickly-excised surgical samples of anesthetized human brain that were flash frozen immediately after removal. Estimated resting in vivo CMR_{glc} based on rates of postmortem metabolite changes in extracts of excised tissue was 0.26 µmol/g/min (Table 4A), similar to that in normal resting adult brain in vivo determined by FDG-PET [68], demonstrating that the in vitro technique was accurate.

The estimated peak glycolytic rate during ischemia (based on disappearance of [glucose + glycogen] and also from the

increase in [lactate] during the first 30 s), rose > 13-fold to 3.4–3.8 µmol/g/min, with an ~ fivefold mean overall increase during the first 5 min. The respective triose flux rates are twice these values (i.e., 2 triose are formed per hexose; Table 4A). In mouse brain, the peak ischemic rise in glycolytic rate was at least 7.4-fold [31], demonstrating that high rates of glucose utilization occur within the first seconds of ischemia in rodent and human brain.

Indirect glycolytic enzyme activities based on measured glucose concentrations in surgically-excised, flash-frozen human brain [34] (Table 3A) and human amino acid levels at zero time (Table 3B) gave dimensionless values for HK–PFK at zero time that are numerically similar to CMR_{glc}, whereas PK was 40% higher; both were less than actual triose flux (Table 4A). Both indirect activities rose ~ 25–30% at 1 min, contrasting the estimated ~ 13-fold peak rate increase immediately after death and the overall fivefold increase during the 0–5 min interval based on measured changes in labile metabolite levels. Indirect activities doubled from 1 to 5 min (Table 4A) when tissue glucose level was ~ 1/3 of the initial value (Table 3A), but both the relative changes and absolute indirect activities at 1 and 5 min were much less than ischemic rate estimates, and indirect values were infinite at 30 min when brain glucose level was zero (Table 4A).

Indirect activities reported by An et al. [5] for HK + PFK and PK (mean group postmortem intervals, 15–17 h; overall range 2–33 h) showed lower values in AD brain for the inferior temporal gyrus, and most PK activities were approximately double HK–PFK (Table 4B). However, these numerical values are much larger than the estimated glucose utilization rates and the corresponding indirect calculated ratios determined at short postmortem times in brain from surgical explants (Table 4A). Serious concerns arise because all brain glucose would be gone within ~ 30 min, yet all postmortem brain glucose levels in the An et al. study are impossibly high (Table 2).

The above comparisons are considered to be only approximate, since indirect ratios are not based on amino acid levels determined in the same tissue samples as glucose concentration. However, the very large differences between indirect estimates of glycolytic activities and rates calculated from changes in metabolite levels within minutes after death reveal the dominant impact of falling glucose concentration and small effect of increases in amino acid levels.

Postmortem Amino Acid Levels Calculated from Reported Glucose Levels and Indirect Glycolytic Enzyme Activities in Control and AD Brain are not Reasonable

Because actual amino acid levels were not reported by An et al. [5], they were estimated by back-calculation from reported HK–PFK activity = ([Ser] + [Gly])/[Glc]. These ratios in inferior temporal gyrus for control and AD are ~ 6.0 and 2.7 (Table 4B) and the respective glucose levels are 476 and 853 µmol/g (Table 2). The corresponding sums of [Ser] + [Gly] are 2856 and 2303 µmol/g for control and AD groups, respectively. Amino acid data are not available for long postmortem intervals in human brain, but at postmortem interval = 4 h, the estimated [Ser] + [Gly] is 2.6 µmol/g (Table 3B). Even if the sum of these amino acids rose by 10-fold at 15–17 h, it would be only 26 µmol/g, ~ 100-fold lower than the derived [Ser] + [Gly] levels. The data cannot be correct.

To sum up, the concentrations of Ser, Gly, and Ala do not reflect their in vivo relative labeling by [^{14}C]glucose (Fig. 1b). Furthermore, calculated indirect ratios relative to glucose level (Table 4A, B) do not correspond to the true net activities of the enzymes, which must be zero at the 15–17 h postmortem intervals for brain harvest due to substrate depletion. Comparison of the measured amino acid and glucose levels in AD brain to those for controls and other diseases reported in the literature should have raised a red flag (Box 1).

Indirect Calculated Enzyme Activities in Postmortem Tissue Compared with Measured Postmortem Enzyme Activities Assayed In Vitro

HK, PFK, and PK activities in living brain are regulated by various effectors, but perhaps the indirect ratio activities may be related to enzyme amount that is proportional to maximal activity in vitro. With the caveat that literature reports of activities of glycolytic enzymes in postmortem AD brain in vitro have been inconsistent, rigorous assays of HK, PFK, and PK specific activities in brain extracts (µmol/min/mg protein) revealed *increases* for PFK and PK activities and *no change* for HK in frontal and temporal cortex of postmortem AD brain compared with age- and premortem severity index-matched controls ([45, 46]; also see the discussion of the cited references in these reports).

Of interest, the sums of the specific activities of HK + PFK for controls and AD brain measured in vitro were ~ 0.26 and 0.31 µmol/min/mg protein, respectively, whereas those for PK were ~ 8.2 and 10.8 µmol/min/mg protein, > 30 times higher than the sum of HK + PFK [45, 46]. In contrast, indirect calculated activities for HK + PFK versus PK based on [amino acid]/[glucose] ratios differed by a factor of ≤ 2 (Table 4). Thus, the ratios calculated as [amino acid]/[glucose] *decrease* in the vulnerable regions of AD brain (inferior temporal gyrus and middle frontal gyrus, Table 4), whereas they *increase* or are *stable* when the relative maximal activities of HK + PFK versus PK in postmortem tissue were assayed under optimal conditions in vitro.

Summary

The use of [amino acid]/[glucose] ratios to evaluate indirectly glycolytic activities in AD and asymptomatic AD subjects was not validated by An et al. [5]. Three different approaches to evaluate the indirect method reveal serious interpretive confounds that arise from the following issues (Box 1): (i) rapid ischemic depletion of the glucose, glycogen, ATP, and PCr metabolic pools; (ii) negligible HK–PFK activities after [PCr] and [ATP] fall to zero, independent of changes in Ser, Gly, and Ala levels; (iii) postmortem autolytic generation of glucose by hydrolysis of carbohydrate moieties of glycolipids and glycoproteins to cause a time-dependent artifactual rise in tissue glucose level; and (iv) catabolism of proteins and peptides to progressively increase amino acid levels with time after death. Beyond 30 min after death, the ratios are driven by postmortem changes, not in vivo regulation of HK, PFK, and PK by various effectors, normal glucose homeostasis, or metabolic dysregulation. Thus, there is no compelling proof that the [amino acid]/[glucose] ratios correctly reflect glycolytic enzyme activities in vitro or fluxes in vivo.

Brain-to-Plasma Glucose Relationships in Normal and AD Brain

It is well known that transport of glucose into brain from blood and into brain cells from extracellular fluid is equilibrative and driven by concentration gradients [71]. Higher concentrations of fasting plasma glucose and greater increases over time were correlated with higher AD brain glucose [5, 58], but the meaning of this association in terms of glucose dysregulation at early stages of AD is not clear. A reason for this uncertainty is the *0.5–17.8 year span* between determination of the last plasma glucose concentration and death. This time interval is so long that it raises some key issues related to interpretation of these findings: the health status of the patients, the time required for brain-plasma glucose equilibration, glucose distribution within brain, the brain:plasma glucose concentration relationship, and neuronal glucose transport.

Take-Home Message

Fundamental properties of brain glucose homeostasis provide an essential perspective for interpretation of levels and correlative associations of plasma and brain glucose concentrations in AD brain. Brain glucose level equilibrates with that in arterial plasma within about an hour, and long-term relationships between plasma and postmortem brain glucose levels are unlikely to be predictive of that in ante mortem diseased brain. Brain glucose levels are relatively homogeneous, and large regional differences in postmortem control brains suggest analytical errors or regional autolytic differences. Extremely high brain glucose levels that exceed plasma levels suggest accumulation of glucose in brain against a concentration gradient, which is impossible because glucose transport is equilibrative.

Equilibration Within ~ 1 h

Brain glucose concentration is the net balance between glucose influx from blood, glucose efflux back to blood, and glucose metabolism in brain. The maximal capacity for glucose transport from plasma to normal human brain exceeds CMR_{glc} by ~ 2.3-fold over a wide range of glucose concentrations and metabolic rates [13, 51, 52, 72], and metabolic modeling predicts (i) neuronal glucose import matches utilization, and (ii) neuronal glucose concentration equals brain glucose level [71].

In rat brain, the half life for glucose is ~ 1.5 min [73], the metabolic glucose pool turns over completely within ~ 10 half lives, and brain glucose equilibrates with plasma glucose within ~ 45–60 min under hypo-, normo- and hyperglycemic conditions in awake and anesthetized rats [74–76]. Glucose turnover in human brain must also be fast, because the brain-plasma equilibration occurs within about an hour under various conditions. For example, when normal humans were given a glucose infusion to raise the plasma level, brain glucose reached a new steady state level within ~ 30–45 min [51, 72]. When Type 1 diabetic patients with hypoglycemic unawareness were subjected to a 30 min hypoglycemic clamp (plasma glucose 2.4 mmol/l) followed by glucose infusion to achieve hyperglycemic-diabetic levels (plasma glucose 16.7 mmol/l), brain levels were modestly but significantly higher in diabetics than in controls, i.e., 5.5 versus 4.7 µmol/g, respectively [77] (compare these values to brain glucose levels in control subjects and AD patients in Table 1). In contrast, normal subjects subjected to three antecedent hypoglycemic episodes within 24 h had similar brain glucose levels during subsequent hyperglycemic infusions as those without preceding hypoglycemia, 5.1 and 4.5 µmol/g, respectively [78]. In both studies, the brain:plasma ratios for glucose were 0.28–0.33 during hyperglycemia. Time course assays during glucose infusion into lean, obese, and Type-2 diabetic subjects showed equilibration to the same elevated plasma level within 60–120 min, but there were small (< ~ 1 mmol/l) but significant differences in the new brain levels among the three groups [79]. Also, the hypothalamic glucose + taurine levels approximately equilibrated with plasma within ~ 70 min at different glucose concentrations (~ 11, 17, and 22 mmol/l) [80].

Thus, normal human and rat brain glucose levels are determined predominantly by plasma glucose levels during the preceding 1–2 h over a wide range of concentrations. Plasma levels are predictive of glucose level in postmortem

brain as long as appropriate procedures are used to obtain the brain tissue, e.g., immediate freezing or microwave fixation to instantly inactivate brain enzymes and stop metabolism. When plasma levels are stable over time, they may be predictive of that in living brain when measured non-invasively by MRS, but plasma levels determined > 0.5 years earlier are unlikely to forecast postmortem brain glucose level. The relationship between ante mortem arterial plasma glucose level and postmortem brain glucose level is very complex, and it is strongly influenced by the agonal stages just prior to death and postmortem ischemia (Box 1). Since the glucose metabolic pool in brain is depleted within 30 min, relationships between antecedent plasma glucose level 6 months earlier and brain glucose at 15–17 h after death are not useful in understanding the pathogenesis of AD.

Regional Brain Glucose Levels

A puzzling finding reported by An et al. [5] is the large range of *control* postmortem glucose levels in the middle frontal gyrus, inferior temporal gyrus, and cerebellum (Table 2). The reported *hexose* concentrations determined by mass spectrometry were assigned to be glucose by An et al. [5], but perhaps autolysis differentially generated hexoses in various brain regions. Based on studies with 3-*O*-methylglucose, glucose is distributed relatively uniformly throughout normal living brain. Methylglucose is a non-metabolizable glucose analog that distributes in brain according to local glucose concentration, and it reveals the homogeneous concentrations of glucose throughout resting rat [63, 81, 82] and human [83] brain. ^{1}H-MRS studies also provide direct evidence that glucose is evenly distributed throughout brain water, with the largest fraction in intracellular space in rat and human brain [72, 84]. There can, of course, be regional differences in glucose concentration in disease states, but the excursions from normal values are quite unlikely to be as large as in the control postmortem brain versus living brain (Tables 1, 2).

Brain: Plasma Glucose Distribution Ratios

The mean fasting plasma glucose levels over a 19 year period in the longitudinal study involving control, asymptomatic AD, and AD subjects (the last sample was an *overall mean* of 5 years prior to death, ranging from 0.5 to 17.8 years) were 5.4, 5.9, and 5.2 mmol/l, respectively (Table 4 of [5]). If these plasma levels were stable until death and using brain levels in Table 2, the respective brain: plasma levels for controls are 113, 88, and 69, and brain/plasma ratios for the AD and asymptomatic AD subjects range from 49 to 164. These extraordinarily high ratios *imply that glucose is concentrated in brain* well above the plasma level. This would require active transport of glucose into brain against its concentration gradient, which is contradicted by a large body of literature cited by Simpson et al. in their review [71]. Values in normo- and hyperglycemic rat and human brain are ~ 0.2–0.3, with an estimate of 0.44 for AD brain. Even if CMR_{glc} were zero, the brain level would passively equilibrate with that in plasma, not accumulate to concentrations 50–160-fold *above* that in plasma. The unrealistically-high brain glucose levels and improbable brain/plasma ratios are two lines of evidence (Box 1) that the brain glucose levels reported by An et al. [5] cannot be correct.

Glucose Transport

Protein concentrations of glucose transporters are proportional to maximal transport capacity (T_{max}) and do not necessarily reflect actual transport rates. Since glucose transport capacity exceeds CMR_{glc}, small changes in transport capacity are unlikely to alter glucose availability to brain cells. An et al. [5] reported that the protein levels of GLUT1 (the endothelial and astrocytic glucose transporter) in postmortem tissue were not different in the middle frontal gyrus of control, AD, and asymptomatic AD subjects (their Fig. 3), indicating that capacity for glucose transport across the blood–brain barrier is not altered by the disease. The neuronal GLUT3 protein level was reduced by ~ 10% in the middle frontal gyrus in AD and asymptomatic AD brain, but this small decrement was not proven to actually reduce neuronal glucose transport.

Recent studies showed that neuronal GLUT4 is mobilized from internal stores to the synaptic plasma membrane during activation to increase glucose transport capacity at the synapse and provide glycolytic ATP for synaptic vesicle recycling [85, 86]. GLUT4 mobilization is also necessary for hippocampal spatial working memory, and amyloidβ(1–42) oligomers impaired insulin signaling, reduced GLUT4 translocation, and caused cognitive impairment [87–89]. If GLUT4 localization is stable at long postmortem intervals, it would be important to evaluate neuronal total and plasma membrane-bound GLUT4 in AD versus controls.

Summary

Long-term associations between plasma and brain glucose levels are of interest and important because they may reflect interactions between peripheral and central glucose homeostasis. However, it is unlikely that this relationship can explain regional differences in brain glucose level in the controls and the extremely high brain glucose levels and tremendously high brain/plasma ratios in all cohorts reported by An et al. [5]. Glucose transport capacity normally exceeds metabolism by a wide margin, it remains to be proven that a 10% decrease in GLUT3 protein would impair neuronal glucose transport. Abnormal

GLUT4 mobilization and levels may contribute to functional and cognitive defects in AD and needs to be evaluated. Indirect calculated glycolytic enzyme activities are very unlikely to be correct, and there is no compelling evidence that "neurons are unable to break down glucose through glycolysis" [58].

Concluding Comments

FDG-PET studies have repeatedly confirmed that reduced CMR_{glc} precedes cognitive decline in AD patients, and in vivo MRS studies indicate that glucose level in AD brain is modestly increased by ~40%, as expected from lower glucose utilization rates. A recent study showed reduced CMR_{O2} in vulnerable regions in subjects with probable AD [90], consistent with mitochondrial abnormalities [69, 91, 92] that include reductions in the α-ketoglutarate dehydrogenase complex in AD and complications arising from mild inhibition of this enzyme (e.g., [93, 94] and cited references). Both glycolytic and oxidative pathway fluxes are affected in AD, but discussion of these issues is beyond the scope of the present review. Because lactate levels in one study ([22], Table 1) are only slightly elevated in AD patients, upregulation of glycolysis does not appear to greatly outstrip oxidative metabolism (with the caveat that lactate efflux to blood was not evaluated), and both pathways may be reduced proportionately. This possibility could be examined by assessment of CMR_{O2}/CMR_{glc} ratios in future PET or MRS studies. The normal resting ratio is close to 6 ($6O_2$ are consumed per glucose oxidized), and it falls when glycolysis is preferentially upregulated with increased lactate production and release. The contributions of specific metabolic steps and of altered cellular functions that, in turn, reduce energy demand, on overall decreases in glucose utilization remain to be established.

This review focuses on the postmortem levels of labile energy metabolites, particularly glucose, in brain of controls and subjects with psychiatric or neurodegenerative disease. Time courses of concentration changes immediately after death have been used to calculate basal and peak ischemic rates of glucose utilization, but, after glucose is rapidly depleted, the ensuing increases in glucose level probably arise from autolytic reactions. Slower, time-varying catabolic activities also alter the concentrations of brain amino acids, and these processes are likely to differ among classes of compounds, disease, and affected brain regions (Box 1). Use of age-, gender-, and postmortem interval-matched samples is essential and critically important, but cannot compensate for the rapid disappearance of brain glucose and other labile energy metabolites within minutes after death. Studies of postmortem human tissue have made major contributions to understanding complex aspects of neurological, psychiatric, and neurodegenerative diseases, but they are not appropriate for study of labile metabolites because postmortem intervals are too long.

Many issues can invalidate extrapolation of postmortem glucose levels to dysregulation of its metabolism in living brain. Some pitfalls can be avoided (Box 1) by reporting absolute levels, not fold-changes or $\log_x$-transformed data. With absolute levels and calculation of brain/plasma ratios, it is readily apparent that the data do not support the conclusion that AD and Huntington's disease patients may be hyperglycemic (postmortem levels are way too low), that brain glucose levels are greatly elevated in association with plasma glucose over the previous decade (levels are much too high), or that there is dysregulation of glycolysis in ante mortem tissue based on ratios of amino acid-to-glucose concentrations (indirect activities cannot be correct because amino acid and glucose levels greatly exceed usual ranges and the indirect enzyme activities reflect postmortem autolysis, not in vivo enzyme activities). When CMR_{glc} and/or glucose transport are affected by disease, it is best to avoid the term 'glucose uptake' that is often used as synonymous with metabolism or utilization. Uptake does not distinguish between glucose transport and glucose phosphorylation, and it does not provide sufficient clarity for readers who must interpret the context of usage.

Future Directions

Many studies with FDG-PET have identified locally-altered CMR_{glc} in AD and other brain disorders, and this method can be used in conjunction with other metabolic assays to evaluate disease progression in living brain. Multi-modal brain PET imaging, ^{1}H-, ^{2}H-, ^{17}O, ^{31}P, and ^{13}C-MRS, and calibrated fMRI technologies can be used non-invasively and longitudinally in vivo to measure metabolite concentrations and metabolic pathway fluxes with variously-labeled substrates, e.g., glucose, ketone bodies, amino acids, or short-chain carboxylic acids [4, 95–98]. In addition, high-field MRS enables in vivo quantification of many brain metabolites [99, 100], and has been used (i) in brain activation studies [15] and (ii) in schizophrenic brain to measure glutamate, GABA, glutamine, and other compounds [101, 102], as well as dysfunction of metabolism and glutamatergic neurotransmission [103]. Calibrated fMRI in AD subjects revealed hypoperfusion and reduced CMR_{O2} in vulnerable brain regions [90], and if this approach were combined with FDG-PET assays of total glucose utilization and [^{13}C]glucose assays of different pathway fluxes in the same subjects, the data may help dissect out altered metabolic steps in diseased brain. Also, resting-state fMRI revealed disruption of the semantic network in patients with mild AD [104]. Thus, rates of oxygen consumption, glucose oxidation, ATP turnover, and excitatory and inhibitory neurotransmitter cycling between astrocytes and neurons can be determined in living brain using these MRS and fMRI techniques, and they can

be applied to patients with neurological diseases who can tolerate the imaging procedures.

Funding This research did not receive any specific grant from funding agencies in the public, commercial, or not-for-profit sectors.

Compliance with Ethical Standards

Conflict of interest The author declares no conflict of interest.

References

1. Sokoloff L (1981) Localization of functional activity in the central nervous system by measurement of glucose utilization with radioactive deoxyglucose. J Cereb Blood Flow Metab 1:7–36
2. Cohen AD, Klunk WE (2014) Early detection of Alzheimer's disease using PiB and FDG PET. Neurobiol Dis 72:117–122
3. Metter EJ, Riege WH, Kameyama M, Kuhl DE, Phelps ME (1984) Cerebral metabolic relationships for selected brain regions in Alzheimer's, Huntington's, and Parkinson's diseases. J Cereb Blood Flow Metab 4:500–506
4. Hyder F, Rothman DL (2017) Advances in imaging brain metabolism. Annu Rev Biomed Eng 19:485–515
5. An Y, Varma VR, Varma S, Casanova R, Dammer E, Pletnikova O, Chia CW, Egan JM, Ferrucci L, Troncoso J, Levey AI, Lah J, Seyfried NT, Legido-Quigley C, O'Brien R, Thambisetty M (2018) Evidence for brain glucose dysregulation in Alzheimer's disease. Alzheimers Dement 14:318–329
6. Duarte JM, Lanz B, Gruetter R (2011) Compartmentalized cerebral metabolism of [1,6-(13)C]glucose determined by in vivo (13)C NMR spectroscopy at 14.1 T. Front Neuroenerget 3:3
7. Gruetter R, Seaquist ER, Ugurbil K (2001) A mathematical model of compartmentalized neurotransmitter metabolism in the human brain. Am J Physiol Endocrinol Metab 281:E100–E112
8. Yoshino Y, Elliott KAC (1970) Incorporation of carbon atoms from glucose into free amino acids in brain under normal and altered conditions. Can J Biochem 48:228–235
9. Reinstrup P, Ståhl N, Mellergård P, Uski T, Ungerstedt U, Nordström C-H (2000) Intracerebral microdialysis in clinical practice: baseline values for chemical markers during wakefulness, anesthesia, and neurosurgery. Neurosurgery 47:701–710
10. Prichard J, Rothman D, Novotny E, Petroff O, Kuwabara T, Avison M, Howseman A, Hanstock C, Shulman R (1991) Lactate rise detected by ^{1}H NMR in human visual cortex during physiologic stimulation. Proc Natl Acad Sci USA 88:5829–5831
11. Hanstock CC, Rothman DL, Prichard JW, Jue T, Shulman RG (1988) Spatially localized ^{1}H NMR spectra of metabolites in the human brain. Proc Natl Acad Sci USA 85:1821–1825
12. Gruetter R, Novotny EJ, Boulware SD, Rothman DL, Mason GF, Shulman GI, Shulman RG, Tamborlane WV (1992) Direct measurement of brain glucose concentrations in humans by ^{13}C NMR spectroscopy. Proc Natl Acad Sci USA 89:1109–1112
13. Gruetter R, Ugurbil K, Seaquist ER (1998) Steady-state cerebral glucose concentrations and transport in the human brain. J Neurochem 70:397–408
14. Mangia S, Tkac I, Gruetter R, Van de Moortele PF, Maraviglia B, Ugurbil K (2007) Sustained neuronal activation raises oxidative metabolism to a new steady-state level: evidence from 1H NMR spectroscopy in the human visual cortex. J Cereb Blood Flow Metab 27:1055–1063
15. Bednarik P, Tkac I, Giove F, DiNuzzo M, Deelchand DK, Emir UE, Eberly LE, Mangia S (2015) Neurochemical and BOLD responses during neuronal activation measured in the human visual cortex at 7 T. J Cereb Blood Flow Metab 35:601–610
16. Boumezbeur F, Petersen KF, Cline GW, Mason GF, Behar KL, Shulman GI, Rothman DL (2010) The contribution of blood lactate to brain energy metabolism in humans measured by dynamic 13C nuclear magnetic resonance spectroscopy. J Neurosci 30:13983–13991
17. Michaelis T, Merboldt KD, Bruhn H, Hanicke W, Frahm J (1993) Absolute concentrations of metabolites in the adult human brain in vivo: quantification of localized proton MR spectra. Radiology 187:219–227
18. Emir UE, Raatz S, McPherson S, Hodges JS, Torkelson C, Tawfik P, White T, Terpstra M (2011) Noninvasive quantification of ascorbate and glutathione concentration in the elderly human brain. NMR Biomed 24:888–894
19. Weaver KE, Richards TL, Logsdon RG, McGough EL, Minoshima S, Aylward EH, Kleinhans NM, Grabowski TJ, McCurry SM, Teri L (2015) Posterior cingulate lactate as a metabolic biomarker in amnestic mild cognitive impairment. Biomed Res Int. https://doi.org/10.1155/2015/610605
20. Moats RA, Ernst T, Shonk TK, Ross BD (1994) Abnormal cerebral metabolite concentrations in patients with probable Alzheimer disease. Magn Reson Med 32:110–115
21. Haley AP, Knight-Scott J, Simnad VI, Manning CA (2006) Increased glucose concentration in the hippocampus in early Alzheimer's disease following oral glucose ingestion. Magn Res Imaging 24:715–720
22. Mullins R, Reiter D, Kapogiannis D (2018) Magnetic resonance spectroscopy reveals abnormalities of glucose metabolism in the Alzheimer's brain. Ann Clin Transl Neurol 5:262–272
23. Ponten U, Ratcheson RA, Salford LG, Siesjo BK (1973) Optimal freezing conditions for cerebral metabolites in rats. J Neurochem 21:1127–1138
24. Veech RL, Harris RL, Veloso D, Veech EH (1973) Freeze-blowing: a new technique for the study of brain in vivo. J Neurochem 20:183–188
25. Fujii T, Hattori K, Miyakawa T, Ohashi Y, Sato H, Kunugi H (2017) Metabolic profile alterations in the postmortem brains of patients with schizophrenia using capillary electrophoresis-mass spectrometry. Schizophr Res 183:70–74
26. Dean B, Thomas N, Scarr E, Udawela M (2016) Evidence for impaired glucose metabolism in the striatum, obtained postmortem, from some subjects with schizophrenia. Transl Psychiatry 6:e949
27. Patassini S, Begley P, Xu J, Church SJ, Reid SJ, Kim EH, Curtis MA, Dragunow M, Waldvogel HJ, Snell RG, Unwin RD, Faull RL, Cooper GJ (2016) Metabolite mapping reveals severe widespread perturbation of multiple metabolic processes in Huntington's disease human brain. Biochim Biophys Acta 1862:1650–1662
28. Xu J, Begley P, Church SJ, Patassini S, McHarg S, Kureishy N, Hollywood KA, Waldvogel HJ, Liu H, Zhang S, Lin W, Herholz K, Turner C, Synek BJ, Curtis MA, Rivers-Auty J, Lawrence CB, Kellett KA, Hooper NM, Vardy ER, Wu D, Unwin RD, Faull RL, Dowsey AW, Cooper GJ (2016) Elevation of brain glucose and polyol-pathway intermediates with accompanying brain-copper deficiency in patients with Alzheimer's disease: metabolic basis for dementia. Sci Rep 6:27524
29. Xu J, Begley P, Church SJ, Patassini S, Hollywood KA, Jullig M, Curtis MA, Waldvogel HJ, Faull RL, Unwin RD, Cooper GJ (2016) Graded perturbations of metabolism in multiple regions of human brain in Alzheimer's disease: snapshot of a pervasive metabolic disorder. Biochim Biophys Acta 1862:1084–1092
30. Graham SF, Holscher C, Green BD (2014) Metabolic signatures of human Alzheimer's disease (AD): 1H NMR analysis of the polar metabolome of post-mortem brain tissue. Metabolomics 10:744–753

31. Lowry OH, Passonneau JV, Hasselberger FX, Schulz DW (1964) Effect of ischemia on known substrates and cofactors of the glycolytic pathway in brain. J Biol Chem 239:18–30
32. Pulsinelli WA, Duffy TE (1983) Regional energy balance in rat brain after transient forebrain ischemia. J Neurochem 40:1500–1503
33. Kerr SE, Ghantus M (1937) The carbohydrate metabolism of brain: III. On the origin of lactic acid. J Biol Chem 117:217–225
34. Kirsch WM, Leitner JW (1967) Glycolytic metabolites and cofactors in human cerebral cortex and white matter during complete ischemia. Brain Res 4:358–368
35. Gümüş A, Gümüş B, Özer E, Yücetaş E, Yücetaş U, Düz E, Sari S, Koldaş M (2016) Evaluation of the postmortem glucose and glycogen levels in hepatic, renal, muscle, and brain tissues: is it possible to estimate postmortem interval using these parameters? J Forensic Sci 61(Suppl 1):S144–S149
36. Perry TL, Hansen S, Gandham SS (1981) Postmortem changes of amino compounds in human and rat brain. J Neurochem 36:406–410
37. Stan AD, Ghose S, Gao XM, Roberts RC, Lewis-Amezcua K, Hatanpaa KJ, Tamminga CA (2006) Human postmortem tissue: what quality markers matter? Brain Res 1123:1–11
38. Toulorge D, Schapira AH, Hajj R (2016) Molecular changes in the postmortem parkinsonian brain. J Neurochem 139(Suppl 1):27–58
39. Jhou JF, Tai HC (2017) The study of postmortem human synaptosomes for understanding Alzheimer's Disease and other neurological disorders: a review. Neurol Ther 6:57–68
40. McCullumsmith RE, Hammond JH, Shan D, Meador-Woodruff JH (2014) Postmortem brain: an underutilized substrate for studying severe mental illness. Neuropsychopharmacology 39:65–87
41. Jové M, Portero-Otín M, Naudí A, Ferrer I, Pamplona R (2014) Metabolomics of human brain aging and age-related neurodegenerative diseases. J Neuropath Exp Neurol 73:640–657
42. Wilkins JM, Trushina E (2018) Application of metabolomics in Alzheimer's disease. Front Neurol 8:719
43. Beach TG, Adler CH, Sue LI, Serrano G, Shill HA, Walker DG, Lue L, Roher AE, Dugger BN, Maarouf C, Birdsill AC, Intorcia A, Saxon-Labelle M, Pullen J, Scroggins A, Filon J, Scott S, Hoffman B, Garcia A, Caviness JN, Hentz JG, Driver-Dunckley E, Jacobson SA, Davis KJ, Belden CM, Long KE, Malek-Ahmadi M, Powell JJ, Gale LD, Nicholson LR, Caselli RJ, Woodruff BK, Rapscak SZ, Ahern GL, Shi J, Burke AD, Reiman EM, Sabbagh MN (2015) Arizona study of aging and neurodegenerative disorders and brain and body donation program. Neuropathology 35:354–389
44. Birdsill AC, Walker DG, Lue L, Sue LI, Beach TG (2011) Postmortem interval effect on RNA and gene expression in human brain tissue. Cell Tissue Bank 12:311–318
45. Bigl M, Bruckner MK, Arendt T, Bigl V, Eschrich K (1999) Activities of key glycolytic enzymes in the brains of patients with Alzheimer's disease. J Neural Transm (Vienna) 106:499–511
46. Bigl M, Bleyl AD, Zedlick D, Arendt T, Bigl V, Eschrich K (1996) Changes of activity and isozyme pattern of phosphofructokinase in the brains of patients with Alzheimer's disease. J Neurochem 67:1164–1171
47. Kerr SE (1936) The carbohydrate metabolism of brain: 1. The determination of glycogen in nerve tissue. J Biol Chem 116:1–7
48. Kerr SE (1935) Studies on the phosphous compounds of brain: I. Phosphocreatine. J Biol Chem 110:625–635
49. Avery BF, Kerr SE, Ghantus M (1935) The lactic acid content of mammalian brain. J Biol Chem 110:637–642
50. Passonneau JV, Hawkins RA, Lust WD, Welsh FA (1980) Cerebral metabolism and neural function. Williams & Wilkins, Baltimore
51. Shestov AA, Emir UE, Kumar A, Henry PG, Seaquist ER, Öz G (2011) Simultaneous measurement of glucose transport and utilization in the human brain. Am J Physiol Endocrinol Metab 301:E1040–E1049
52. de Graaf RA, Pan JW, Telang F, Lee JH, Brown P, Novotny EJ, Hetherington HP, Rothman DL (2001) Differentiation of glucose transport in human brain gray and white matter. J Cereb Blood Flow Metab 21:483–492
53. Holden JE, Mori K, Dienel GA, Cruz NF, Nelson T, Sokoloff L (1991) Modeling the dependence of hexose distribution volumes in brain on plasma glucose concentration: implications for estimation of the local 2-deoxyglucose lumped constant. J Cereb Blood Flow Metab 11:171–182
54. Gandhi GK, Ball KK, Cruz NF, Dienel GA (2010) Hyperglycaemia and diabetes impair gap junctional communication among astrocytes. ASN Neuro 2:e00030
55. Jedziniak JA, Chylack LT Jr, Cheng HM, Gillis MK, Kalustian AA, Tung WH (1981) The sorbitol pathway in the human lens: aldose reductase and polyol dehydrogenase. Invest Ophthalmol Vis Sci 20:314–326
56. Giacco F, Brownlee M (2010) Oxidative stress and diabetic complications. Circ Res 107:1058–1070
57. Boretius S, Tammer R, Michaelis T, Brockmöller J, Frahm J (2013) Halogenated volatile anesthetics alter brain metabolism as revealed by proton magnetic resonance spectroscopy of mice in vivo. NeuroImage 69:244–255
58. Talan J (2017) In the pipeline-Alzheimer's disease: new evidence for brain glucose dysregulation in Alzheimer's disease abnormalities evident years before clinical symptoms. Neurol Today 17:7–8
59. Nordström CH, Nielsen TH, Jacobsen A (2013) Techniques and strategies in neurocritical care originating from southern Scandinavia. J Rehabil Med 45:710–717
60. Kirsch WM, Schulz Q, Van Buskirk J, Nakane P (1972) Anaerobic energy metabolism in brain tumors. Prog Exp Tumor Res 17:163–191
61. Kirsch WM, Leitner JW (1967) A comparison of the anaerobic glycolysis of human brain and glioblastoma. J Neurosurg 27:45–51
62. Kirsch WM (1965) Substrates of glycolysis in intracranial tumors during complete ischemia. Cancer Res 25:432–439
63. Sokoloff L, Reivich M, Kennedy C, Des Rosiers MH, Patlak CS, Pettigrew KD, Sakurada O, Shinohara M (1977) The [^{14}C] deoxyglucose method for the measurement of local cerebral glucose utilization: theory, procedure, and normal values in the conscious and anesthetized albino rat. J Neurochem 28:897–916
64. Sims NR, Bowen DM, Davison AN (1981) [^{14}C]acetylcholine synthesis and [^{14}C]carbon dioxide production from [U-^{14}C] glucose by tissue prisms from human neocortex. Biochem J 196:867–876
65. Sims NR, Bowen DM, Smith CC, Flack RH, Davison AN, Snowden JS, Neary D (1980) Glucose metabolism and acetylcholine synthesis in relation to neuronal activity in Alzheimer's disease. Lancet 1:333–336
66. Sims NR, Bowen DM, Allen SJ, Smith CC, Neary D, Thomas DJ, Davison AN (1983) Presynaptic cholinergic dysfunction in patients with dementia. J Neurochem 40:503–509
67. Sims NR, Bowen DM, Neary D, Davison AN (1983) Metabolic processes in Alzheimer's disease: adenine nucleotide content and production of $^{14}CO_2$ from [U-^{14}C]glucose in vitro in human neocortex. J Neurochem 41:1329–1334
68. Hyder F, Herman P, Bailey CJ, Moller A, Globinsky R, Fulbright RK, Rothman DL, Gjedde A (2016) Uniform distributions of glucose oxidation and oxygen extraction in gray matter of normal human brain: no evidence of regional differences of aerobic glycolysis. J Cereb Blood Flow Metab 36:903–916
69. Swerdlow R, Marcus DL, Landman J, Kooby D, Frey W 2nd, Freedman ML (1994) Brain glucose metabolism in Alzheimer's disease. Am J Med Sci 308:141–144

70. Dienel GA, Wang RY, Cruz NF (2002) Generalized sensory stimulation of conscious rats increases labeling of oxidative pathways of glucose metabolism when the brain glucose-oxygen uptake ratio rises. J Cereb Blood Flow Metab 22:1490–1502
71. Simpson IA, Carruthers A, Vannucci SJ (2007) Supply and demand in cerebral energy metabolism: the role of nutrient transporters. J Cereb Blood Flow Metab 27:1766–1791
72. Gruetter R, Novotny EJ, Boulware SD, Rothman DL, Shulman RG (1996)) ^{1}H NMR studies of glucose transport in the human brain. J Cereb Blood Flow Metab 16:427–438
73. Savaki HE, Davidsen L, Smith C, Sokoloff L (1980) Measurement of free glucose turnover in brain. J Neurochem 35:495–502
74. Mori K, Cruz N, Dienel G, Nelson T, Sokoloff L (1989) Direct chemical measurement of the lambda of the lumped constant of the [^{14}C]deoxyglucose method in rat brain: effects of arterial plasma glucose level on the distribution spaces of [^{14}C]deoxyglucose and glucose and on lambda. J Cereb Blood Flow Metab 9:304–314
75. Choi IY, Lei H, Gruetter R (2002) Effect of deep pentobarbital anesthesia on neurotransmitter metabolism in vivo: on the correlation of total glucose consumption with glutamatergic action. J Cereb Blood Flow Metab 22:1343–1351
76. Duarte JMN, Gruetter R (2012) Characterization of cerebral glucose dynamics in vivo with a four-state conformational model of transport at the blood–brain barrier. J Neurochem 121:396–406
77. Criego AB, Tkac I, Kumar A, Thomas W, Gruetter R, Seaquist ER (2005) Brain glucose concentrations in patients with type 1 diabetes and hypoglycemia unawareness. J Neurosci Res 79:42–47
78. Criego AB, Tkac I, Kumar A, Thomas W, Gruetter R, Seaquist ER (2005) Brain glucose concentrations in healthy humans subjected to recurrent hypoglycemia. J Neurosci Res 82:525–530
79. Hwang JJ, Jiang L, Hamza M, Sanchez Rangel E, Dai F, Belfort-DeAguiar R, Parikh L, Koo BB, Rothman DL, Mason G, Sherwin RS (2017) Blunted rise in brain glucose levels during hyperglycemia in adults with obesity and T2DM. JCI Insight. https://doi.org/10.1172/jci.insight.95913
80. Seaquist ER, Moheet A, Kumar A, Deelchand DK, Terpstra M, Kubisiak K, Eberly LE, Henry PG, Joers JM, Oz G (2017) Hypothalamic flucose transport in humans during experimentally induced hypoglycemia-associated autonomic failure. J Clin Endocrinol Metab 102:3571–3580
81. Gjedde A, Diemer NH (1983) Autoradiographic determination of regional brain glucose content. J Cereb Blood Flow Metab 3:303–310
82. Nakanishi H, Cruz NF, Adachi K, Sokoloff L, Dienel GA (1996) Influence of glucose supply and demand on determination of brain glucose content with labeled methylglucose. J Cereb Blood Flow Metab 16:439–449
83. Gjedde A, Wienhard K, Heiss WD, Kloster G, Diemer NH, Herholz K, Pawlik G (1985) Comparative regional analysis of 2-fluorodeoxyglucose and methylglucose uptake in brain of four stroke patients. With special reference to the regional estimation of the lumped constant. J Cereb Blood Flow Metab 5:163–178
84. Pfeuffer J, Tkac I, Gruetter R (2000) Extracellular-intracellular distribution of glucose and lactate in the rat brain assessed noninvasively by diffusion-weighted 1H nuclear magnetic resonance spectroscopy in vivo. J Cereb Blood Flow Metab 20:736–746
85. Ashrafi G, Wu Z, Farrell RJ, Ryan TA (2017) GLUT4 mobilization supports energetic demands of active synapses. Neuron 93:606–615.e603
86. Ashrafi G, Ryan TA (2017) Glucose metabolism in nerve terminals. Curr Opin Neurobiol 45:156–161
87. Pearson-Leary J, McNay EC (2012) Intrahippocampal administration of amyloid-beta(1–42) oligomers acutely impairs spatial working memory, insulin signaling, and hippocampal metabolism. J Alzheimers Dis 30:413–422
88. Pearson-Leary J, McNay EC (2016) Novel roles for the insulin-regulated glucose transporter-4 in hippocampally dependent memory. J Neurosci 36:11851–11864
89. Pearson-Leary J, Jahagirdar V, Sage J, McNay EC (2018) Insulin modulates hippocampally-mediated spatial working memory via glucose transporter-4. Behav Brain Res 338:32–39
90. Lajoie I, Nugent S, Debacker C, Dyson K, Tancredi FB, Badhwar A, Belleville S, Deschaintre Y, Bellec P, Doyon J, Bocti C, Gauthier S, Arnold D, Kergoat MJ, Chertkow H, Monchi O, Hoge RD (2017) Application of calibrated fMRI in Alzheimer's disease. Neuroimage Clin 15:348–358
91. Swerdlow RH (2016) Bioenergetics and metabolism: a bench to bedside perspective. J Neurochem 139(Suppl 2):126–135
92. Swerdlow RH (2018) Mitochondria and mitochondrial cascades in Alzheimer's disease. J Alzheimers Dis 62:1403–1416
93. Chen H, Denton TT, Xu H, Calingasan N, Beal MF, Gibson GE (2016) Reductions in the mitochondrial enzyme alpha-ketoglutarate dehydrogenase complex in neurodegenerative disease - beneficial or detrimental? J Neurochem 139:823–838
94. Banerjee K, Munshi S, Xu H, Frank DE, Chen HL, Chu CT, Yang J, Cho S, Kagan VE, Denton TT, Tyurina YY, Jiang JF, Gibson GE (2016) Mild mitochondrial metabolic deficits by alpha-ketoglutarate dehydrogenase inhibition cause prominent changes in intracellular autophagic signaling: potential role in the pathobiology of Alzheimer's disease. Neurochem Int 96:32–45
95. Mason GF, Petersen KF, de Graaf RA, Shulman GI, Rothman DL (2007) Measurements of the anaplerotic rate in the human cerebral cortex using 13C magnetic resonance spectroscopy and [1-^{13}C] and [2-^{13}C] glucose. J Neurochem 100:73–86
96. Patel AB, de Graaf RA, Mason GF, Rothman DL, Shulman RG, Behar KL (2005) The contribution of GABA to glutamate/glutamine cycling and energy metabolism in the rat cortex in vivo. Proc Natl Acad Sci USA 102:5588–5593
97. Zhu XH, Lu M, Chen W (2018) Quantitative imaging of brain energy metabolisms and neuroenergetics using in vivo X-nuclear (2)H, (17)O and (31)P MRS at ultra-high field. J Magn Reson 292:155–170
98. Zhu XH, Lee BY, Chen W (2018) Functional energetic responses and individual variance of the human brain revealed by quantitative imaging of adenosine triphosphate production rates. J Cereb Blood Flow Metab 38:959–972
99. Henning A (2018) Proton and multinuclear magnetic resonance spectroscopy in the human brain at ultra-high field strength: a review. Neuroimage 168:181–198
100. Zhang N, Song X, Bartha R, Beyea S, D'Arcy R, Zhang Y, Rockwood K (2014) Advances in high-field magnetic resonance spectroscopy in Alzheimer's disease. Curr Alzheimer Res 11:367–388
101. Thakkar KN, Rosler L, Wijnen JP, Boer VO, Klomp DW, Cahn W, Kahn RS, Neggers SF (2017) 7T Proton magnetic resonance spectroscopy of gamma-aminobutyric acid, glutamate, and glutamine reveals altered concentrations in patients with schizophrenia and healthy siblings. Biol Psychiatry 81:525–535
102. Brandt AS, Unschuld PG, Pradhan S, Lim IA, Churchill G, Harris AD, Hua J, Barker PB, Ross CA, van Zijl PC, Edden RA, Margolis RL (2016) Age-related changes in anterior cingulate cortex glutamate in schizophrenia: A (1)H MRS study at 7 T. Schizophr Res 172:101–105
103. Duarte JMN, Xin L (2018) Magnetic resonance spectroscopy in schizophrenia: evidence for glutamatergic dysfunction and impaired energy metabolism. Neurochem Res. https://doi.org/10.1007/s11064-11018-12521-z
104. Mascali D, DiNuzzo M, Serra L, Mangia S, Maraviglia B, Bozzali M, Giove F (2018) Disruption of semantic network in mild Alzheimer's disease revealed by resting-state fMRI. Neuroscience 371:38–48